ZINC OXIDE NANOPARTICLES AS POTENTIAL NOVEL ANTICANCER THERAPIES

by

Janet C. Layne

A thesis

submitted in partial fulfillment

of the requirements for the degree of

Master of Science in Biology

Boise State University

May 2011

BOISE STATE UNIVERSITY GRADUATE COLLEGE

DEFENSE COMMITTEE AND FINAL READING APPROVALS

of the thesis submitted by

Janet C. Layne

Thesis Title: Zinc Oxide Nanoparticles as Potential Novel Anticancer Therapies

Date of Final Oral Examination: 10 December 2010

The following individuals read and discussed the thesis submitted by student Janet C. Layne, and they also evaluated her presentation and response to questions during the final oral examination. They found that the student passed the final oral examination, and that the thesis was satisfactory for a master's degree and ready for any final modifications that they explicitly required.

Denise Wingett, Ph.D.	Chair, Supervisory Committee
Kevin Feris, Ph.D.	Member, Supervisory Committee
Alex Punnoose, Ph.D.	Member, Supervisory Committee
Juliette Tinker, Ph.D.	Member, Supervisory Committee

The final reading approval of the thesis was granted by Denise Wingett, Ph.D., Chair of the Supervisory Committee. The thesis was approved for the Graduate College by John R. Pelton, Ph.D., Dean of the Graduate College.

DEDICATION

For my parents, Kathryn Newman and Michael Jones, and my fiancé Oscar; without them I couldn't have done this.

ACKNOWLEDGEMENTS

I must first and foremost show my gratitude to my thesis advisor, Dr. Denise Wingett, whose encouragement, knowledge, and willingness to avail herself to assist me at all times were paramount to the success of this thesis. Secondly, I would like to acknowledge the members of my thesis committee. Dr. Alex Punoose, who spearheaded the BSU nanobiology project, was also immensely helpful, both in clarifying convoluted physics topics, and in providing unfailing optimism and leadership to all involved. For those contributions and more I am truly grateful. I owe many thanks to Dr. Kevin Feris for lending his knowledge and expertise, and for sending suggestions and helpful literature my way. I must also acknowledge Dr. Juliette Tinker, for bringing helpful suggestions to the nano group, for joining my committee, and taking time in her busy schedule to edit my thesis.

In addition to their service as committee members, I must also thank Dr. Alex Punoose, Dr. Kevin Feris, and Dr. Denise Wingett for their contributions toward the authorship of Chapter 2 of this thesis.

I would like to show my appreciation to Dr. Alex Punoose's Physics lab, Aaron Thurber in particular, for manufacturing all of the nanoparticles used in this work.

Several fellow members of my lab, past and present, are deserving of thanks, including Ashley Masterson and Dr. John Rasmussen for their suggestions, help in day-to day lab functions, and, importantly, their camaraderie. Special thanks must go to Panagiota Louka, for her red blood cell viability data in Figure 3.2A and to Ezequiel Martinez, for his data on erythroleukemia cell viability in Figure 3.2B. I owe to Cory Hanley my deepest gratitude for countless contributions to this work. She contributed authorship to Chapter 2 of this thesis, as well as the primary T and B cell data in Figures 2.1, 2.3, 2.4, and 2.6A, and spent countless hours training me and assisting with blood draws and T cell isolations. Importantly, her familiarity with my thesis allowed her to be a sounding board for result interpretation, frustrations, new ideas, and to be optimally effective in providing suggestions to improve experimental design. In Cory, I also found a lifelong friend, for which I am truly grateful.

I give my sincerest thanks to all those mentioned here, for their help with my thesis, and for their part in making my graduate school experience a happy one.

ABSTRACT

Nanoparticles (NP) are increasingly being recognized for their utility in the field of medicine, including use as drug carriers and imaging tools. We demonstrated that ZnO NP preferentially kill cancerous cells of the T cell lineage, and extended this research to evaluate other cells types, including normal and malignant B cells, and normal and malignant breast and prostate epithelial cells. Preferential ZnO nanoparticle cytotoxicity occurred for multiple types of cancer cells, but was most pronounced for non-adherent cells of hematopoietic lineage. Normal T and B lymphocytes showed the greatest resistance to NP toxicity, followed by normal breast epithelial cells, and appeared to be closely tied to cellular proliferative potential. Reactive oxygen species generation contributed, at least in part, towards cancer cell selectivity with greater levels of reactive oxygen species being induced in cancerous cells compared to normal cell counterparts. The extracellular dissolution of ZnO NP did not appear to appreciably contribute to the toxicity mechanism, and endocytosis of nanoparticles appeared to be required for toxicity. Particle charge was found to have an effect on toxicity, with more cationic nanoparticles having a greater toxicity than neutral/anionic particles, and may be an important factor in future studies aimed at improving cancer cell selectivity. Overall, these findings suggest that ZnO nanoparticles may have utility in anticancer regimens aimed at hematological malignancies.

TABLE OF CONTENTS

LIST OF TABLES

LIST OF FIGURES

LIST OF ABBREVIATIONS

$\cdot O_2^-$	superoxide
$\cdot OH^-$	hydroxyl radical
µg	microgram
µL	microliter
µM	micromolar
ADP	Adenosine diphosphate
Al_2O_3	Aluminum oxide
ATP	Adenosine triphosphate
CdSe	Cadmium selenide
CeO	Cerium oxide
CNT	carbon nanotubes
CO_2	carbon dioxide
DCFH-DA	2,7-dichlorofluorescein diacetate
DEG	Diethylene glycol
DNA	Deoxyribonucleic acid

EGF	Epidermal growth factor
EGFR	Epidermal growth factor receptor
EPR	Enhanced permeation and retention
FBS	Fetal Bovine Serum
Fe_2O_3	Iron oxide
FGF	Fibroblast growth factor
FITC	fluorescein isothiocyanate
FS	forward scatter
g	gram
GDP	Guanosine diphosphate
Glth	Glutathione
GPCR	G-protein coupled receptor
GPI	glycosylphosphatidylinositol
GRAS	Generally Recognized as Safe
GTP	Guanosine triphosphate
h	hours
Hsc70	Heat shock cognate 70

IGF	Insulin like growth factor
kg	kilogram
L	liter
LD_{50}	Lethal dose 50%
LDH	lactate dehydrogenase
MFI	mean fluorescence intensity
mg	milligram
mM	millimolar
MSDS	Material Safety Data Sheet
NAC	N-Acetyl Cysteine
NADH	nicotinamide adenine dinucleotide
NCI	National Cancer Institute
ng	nanogram
nm	nanometer
NP	nanoparticles
O_2	molecular oxygen
PBMC	Peripheral blood mononuclear cells

PBS	Phosphate Buffered Saline
PDT	Photodynamic therapy
PEG	polyethylene glycol
PI	Propidium iodide
PMA	Phorbol 12-Myristate 13-Acetate
pRb	Retinoblastoma protein
RBC	red blood cell
RES	reticuloendothelial system
RNA	Ribonucleic acid
ROS	Reactive oxygen species
RTK	Receptor tyrosine kinase
SiO_2	Silicon dioxide
SSC	side scatter
TEM	Transmission electron microscopy
TGF-α	Transforming growth factor alpha
TiO_2	Titanium dioxide
UV	Ultraviolet

VEGF	Vascular endothelial growth factor
XRD	X ray diffraction
$ZnCl_2$	Zinc chloride
ZnO	Zinc oxide
ZnS	Zinc sulfide
$ZnSO_4$	Zinc sulfate

CHAPTER 1: INTRODUCTION

Advancements in materials science and the ever-increasing miniaturization of technology have led to the development of nanotechnology, a discipline concerned with the development and utilization of nanomaterials, structures with dimensions in the 1-100 nm range. These nanomaterials have found a large niche in the field of biotechnology for a variety of reasons. Their size is comparable to biological molecules, making them more penetrant than larger substances and ideally-sized for interactions with cellular structures (McNeil, 2005). Reduction of materials to the nanometer scale can alter physical, chemical, and quantum properties that can potentially be exploited for imaging and treating diseased cells. Surface area to volume ratio increases steeply with the reduction of NP size, resulting in greater surface reactivity (Nel et al., 2006). Discovery of these new properties has sparked intense research into biological interactions with nanomaterials, both for their potential toxicity to biological systems and their potential utility in medical applications.

Nanotechnology and Nanomaterials

Nanotechnology is broadly defined as the manipulation of matter on a molecular scale. This refers to the production of structures and even devices, called nanomaterials, in the size range of 1 to 100 nm in any dimension (Nel et al., 2006). The ever-increasing demand for the miniaturization of technology has resulted in an explosion in nanotechnology research and products containing nanomaterials. According to the Project

on Emerging Nanotechnologies, a website devoted to creating inventories of nanotechnology uses, as of August 2009, there existed 1,015 products containing nanomaterials, up 379% from 2006 (2010). The range in use of these products is wide; nanotechnology has made its way into cosmetics, sunscreen, clothing, electronics, appliances, filtration, medicine, and even food products (Sozer and Kokini, 2009; Project on Emerging Nanotechnologies, 2010). Silver nanoparticles (NP) are currently the most heavily used, being incorporated for their antimicrobial properties in clothing, upholstery, pillows, food storage containers, and even toys for children (Schrand et al., 2010; Project on Emerging Nanotechnologies, 2010).

In 1959, physicist Richard Feynman gave a talk at the American Physical Society entitled "There's Plenty of Room at the Bottom" in which he discussed the possibilities of directly manipulating single atoms and molecules in structures. He also highlighted that these materials may behave differently on such a small scale. For instance, gravity would hold less sway, while Van der Waals forces would become more important (Feynman, 1960). This lecture had little effect over the subsequent 20 years, but has been looked at in hindsight as that which sparked the move toward nanotechnology development that now encompasses different types of nanomaterials utilized in many different areas.

Though the physical and chemical properties of substances have been well characterized, an intriguing facet of nanotechnology is that materials reduced to the nanoscale in size begin to display different physical and chemical properties. This can include changes in optical properties, such as color and light diffraction, solubility,

hardness and strength, magnetism, heat, and electrical conductivity, and surface reactivity (Schrand et al., 2010). As NP size is reduced, the surface area-to-volume ratio increases, and a large number of the atoms composing the particle are found on the particle surface (Nel et al., 2006). This can render substances previously thought inert suddenly highly reactive. These changes in properties mean that researchers cannot rely upon expectations of chemical behavior based upon the previously understood characteristics of these substances. This has profound impacts upon toxicology; it cannot be assumed that substances that are safe on the bulk (micron) scale will be so when reduced to nano size. Different properties also open new doors for utility, and are being exploited for applications such as imaging and cosmetics.

Different types of nanomaterials are now being synthesized from a variety of different substances. Carbon nanotubes (CNT) are studied heavily due to their strength, hardness, heat, and electrical conductivity (Lacerda et al., 2006). Scientists have found that carbon nanotubes can be engineered harder than diamonds, and are looking at them with increasing interest as scaffolds for tissue regeneration (Blank et al., 1998; Saito et al., 2009). Many other substances including gold, silver, and semiconducting materials such as metal oxides have also been used to form nanorods and NP (Schrand et al., 2010). Nanoparticles are those with diameters of 1-100 nm, and those made of semiconducting materials sized approximately 10 nm or less behave as quantum dots, in which the band gap can be modified with NP size (Medintz et al., 2005). The band gap is the amount of energy required for an electron in the material to be liberated from the allowed valence band and become a charge carrier. If enough energy is supplied, an electron jumps from

the valence band to the conductance band, leaving behind a vacancy called an electron "hole" in the valance band (Mansur, 2010). In NP, a large portion of the atoms are found at the surface, and consequently so too are the highly reactive valence electrons and holes. This has strong implications for the potential of NP to have toxic reactivity in biological systems.

Toxicology of Nanoparticles

People come into contact with many chemical substances in a variety of ways, often purposefully, though unknowingly, through the products that they use every day. It is assumed that anything readily available to the public has undergone rigorous testing before it is cleared for use, and usually this is true. For instance, toxicological studies for substances that may be used as food additives are overseen and compiled by the Federal Drug Administration, who maintains a list of those "Generally Recognized as Safe". If a substance is considered GRAS, it has been shown through rigorous *in vitro* and *in vivo* experiments to be nontoxic, or has been used for a great number of years with no known negative effects. Once included in the GRAS list, a chemical is acceptable for use as a food additive and is thereafter not expected to prove nontoxic before use (2006). Products have appeared in recent years that contain NP assumed to be safe because the bulk forms of the chemicals are nontoxic. Given that materials can take on entirely different properties when reduced to the nanoscale, and their potential to penetrate more deeply into tissues and cells, this may not be a correct assumption (Nel et al., 2006).

Metal oxide NP include materials such as TiO_2, CeO_2, Al_2O_3, Fe_2O_3, and ZnO, and are already found in many products. TiO_2 and ZnO nanomaterials are used in topically applied products such as sunscreens and cosmetics, as are pure gold NP. These nanomaterials were incorporated into consumer products on the assumption that they would be non-toxic, like their bulk counterparts, but studies have found that this is not necessarily true. ZnO NP, in particular, have been found to demonstrate strikingly different toxicological profiles *in vitro* than bulk ZnO (Reddy et al., 2007; Jiang et al., 2009). It is for this reason that this work focuses on NP of ZnO over other nanomaterials.

Zinc oxide is an inorganic white powder that is very poorly soluble in water. It is a semiconducting material, and is used as an additive in many products, including plastics, rubber, glass, paint, and even food as a source of zinc. ZnO has a lethal dose (LD_{50}) in mice of 7,950 mg/kg, making it relatively nontoxic (Material Safety Data Sheet: ZnO). Based upon this lack of toxicity, ZnO NP, assumed to be equally safe, began replacing bulk powder in certain products. Because particulate ZnO is more transparent than the bulk form but retains its ability to reflect UV light, it has become common practice to use ZnO NP in sunscreens and cosmetics. This has raised questions in the public arena and sparked detailed research into the *in vitro* toxicity of many metal oxide NP (Nel et al., 2006). Research in prokaryotic organisms showed that Al_2O, SiO_2, and ZnO were all significantly more toxic to *E. coli*, *B. subtilis*, and *P. fluorescens* in NP form, with ZnO being the most toxic (Jiang et al., 2009). Another study found similar results with ZnO NP in primary human T cells (Reddy et al., 2007). This apparent

increase in toxicity necessitates further exploration into the interactions of ZnO NP in relevant biological systems.

Zinc oxide is a crystalline semiconducting material with its electrons contained in discrete energy bands, and exhibits quantum confinement at nanoscale. The highest electron-containing band is the valence band, while the lowest empty band is called the conductance band. When sufficient energy is supplied, an electron is able to jump from the valence to the conductance band, which means it is liberated from chemical bonds and may act as a mobile charge carrier (Mansur, 2010). Conductance band electrons will act as powerful reductants in aqueous solutions, and can donate electrons to oxygen to generate superoxide radicals. The electron vacancies or holes left behind when the electron moves into the conductance band can also act as powerful oxidants in water. One study showed that quantum dot-sized ZnO was capable of photocatalyzing the production in water of hydrogen peroxide, a species of reactive oxygen, 100-1000 times faster than bulk ZnO (Hoffman et al., 1994). This was believed to occur due to the greater surface area to volume ratio of NP, the resultant greater number of reactive sites at the surface, and the greater number of surface impurities found in NP capable of "trapping" the electrons and holes at the surface (Hoffman et al., 1994; Sharma et al., 2009). Another study discusses this same electron-trapping at the nanoparticle surface as a mechanism for the generation of reactive oxygen in the absence of photocatalysis (Yang et al., 2009). For this reason, ZnO in NP form may be more capable of participating in redox cycling in aqueous or even oxygen-containing environments (e.g., cells) and producing reactive oxygen species. Many studies have shown that the toxicity of NP of various types is

mediated by oxidative stress in cells, and that ZnO NP are capable of ROS induction both in abiotic and biotic systems (Xia et al., 2008). This ability to redox cycle and create reactive oxygen species in water is likely responsible for the greater toxicity that ZnO NP display over micron-sized ZnO materials.

Nanomedicine

With products containing NP on the rise, not only is there a need to understand their toxicity, but to fully assess the potential for novel biological uses. Nanomedicine refers to the usage of nanotechnology in medical applications. While the study is very new, many promising utilizations have emerged in this field. Some of the unique properties of nanomaterials have already proven useful in biological applications. For instance, NP are on the same size scale as biological molecules, and so are better able to penetrate tissues and cells and interact with these structures where larger molecules are limited (McNeil, 2005). The surface reactivity of NP makes them easy to modify, either through the addition of drugs or targeting molecules to direct them to specific cell or tissue types (Nel et al., 2006).

Current research in the field of nanomedicine has focused on the use of NP as imaging agents or drug carriers of existing therapeutics. Quantum dots in particular have been extensively researched because their fluorescent emissions can be altered simply by changing NP size (through band gap enlargement) and they have broadened excitation spectra. This means that a variety of different-sized NP (therefore fluorescing at different wavelengths), targeted to different cells or tissues, can be excited simultaneously with the

same light source. These quantum dots also show high resistance to photo and chemical degradation, unlike organic dyes currently in use. Inorganic quantum dots can also be conjugated with biological molecules such as DNA and proteins, which allows the structure to be targeted biologically and fluoresce (Medintz et al., 2005). One group found that by conjugating ZnS-capped CdSe quantum dots with homing peptides, they were able to cause accumulation in the lungs and in blood or lymphatic vessels in tumors in mice (Akerman et al., 2002). They were also able to avoid clearance by the reticuloendothelial system (RES) by adding a polyethylene glycol (PEG) coating to the NP (Akerman et al., 2002). Other studies have found that adsorption or encapsulation of DNA-based vaccines onto/ into NP enhances their ability to induce immunity through the protection of DNA degradation and increased uptake (Xiang et al., 2010).

Magnetofection is a new technique that involves delivery of DNA to cells using nontoxic magnetic NP. The application uses DNA adsorbed onto magnetic NP that are then targeted to cells by applying an external magnetic field (Plank et al., 2003). Magnetic NP have also shown promise in the area of drug delivery, as they can be targeted to desired areas in the body (Sun et al., 2008). Liposomes are another heavily researched nanomedicine, used as drug delivery agents. These are artificial nano-sized lipid bilayers engineered to contain a drug to be delivered to a target site including tumors (Kaasgaard, and Adresen, 2010). Nanomedicine has focused particularly on cancer treatment in an attempt to find more efficacious treatments that are simultaneously better tolerated by patients. Overall, NP have demonstrated novel potential and wide-ranging utility in medical applications, and research is ongoing. The future of medicine looks to be tightly entwined with that of nanotechnology.

Cancer

Epidemiology and Cost

Cancer is a term used to describe a diverse group of diseases hallmarked by uncontrolled proliferation, tissue invasion, and often metastasis. According to the World Health Organization, it is one of the most prominent causes of death, killing 7.4 million people worldwide in the year 2004. This number is expected to rise to approximately 12 million by 2030. In America alone, approximately 44% of men and 38% of women will develop some form of cancer in their lifetime, and about 23% of American men and 20% of American women will die from some form of cancer (Altekruse et al., 2010). The health care cost in the United States in 2006 for treatment alone was $104.1 billion according to the National Cancer Institute's publication Cost of Cancer Care (NCI, 2010). Substantial amounts of money are also spent on cancer research; according to their statistics on research funding the National Cancer Institute alone currently budgets approximately $4.8 billion annually, and contributions from private, for-profit companies (Big Pharma) equals that amount at least (de Francisco and Matlin, 2006; NCI, 2010). This makes the search for inexpensive, safe, and effective treatments a high priority for biomedical researchers.

Classification

Cancer can arise in all cell types and is classified by the lineage of the original transformed cell. Epithelial cells are found covering the body's surfaces and lining the internal organs and cavities. Cells of this type that give rise to cancer are classified as

carcinomas. These are the most common types of cancer; they make up most breast, prostate, and lung cancers (Roomi et al., 2009). Cells of the hematopoeitic lineage are those that originate in the bone marrow and include erythrocytes and the white blood cells of the immune system. Cancers that arise in this lineage are classified as leukemias and lymphomas. Leukemias arise in cells in the bone marrow and result in malignant cells circulating in the bloodstream, while lymphomas occur in immune cells of the lymphatic system (Leukemia and Lymphoma Society). Sarcomas typically are cancers that originate from connective tissues such as bone, cartilage, muscle, deep skin, or fat, although some cancers of epithelial origin have been classified here (Jain et al., 2010). Most malignancies result in the formation of solid masses of transformed cells called tumors, though leukemias do not. This work will mainly focus upon carcinomas, leukemias and lymphomas, though future work will include sarcomas.

Symptoms and Causes

The ability of cancer to affect a large variety of cell types makes its symptom profile very diverse. Solid tumors can invade and compress surrounding tissues, leading to disruption of the functioning of body tissues and organs. Local symptoms can include swelling, pain, and jaundice. Systemic symptoms are more invasive; weight loss, fatigue, wasting, and anemia are common to most cancers, and cancer type-specific symptoms can also occur. In addition, metastases can cause yet another set of symptoms, including enlarged liver, bone pain, and neurological symptoms (Greenberg et al., 1964; NCI, 2006). Alongside the symptoms of cancer, treatments often exhibit a multitude of negative side effects, discussed in detail later in this chapter.

Cancer is caused by an accumulation of damage to the DNA of cells that leads to the deactivation of tumor suppressor genes and/or activation of oncogenes. Oncogenes are those that govern the ability of the cell to rapidly divide and proliferate, while tumor suppressor genes are those that in normal cells prevent the excessive growth and invasion of tissues (Rhim, 1988). Oncogenes include transcription factors or regulatory GTPases that regulate proliferation, Receptor Tyrosine Kinases that, when mutated, render growth factor receptors constitutively active, genes that cause cells to abnormally secrete growth factors, or genes that confer protection from apoptosis (Croce, 2008). Tumor suppressor genes include those that inhibit cell cycling, promote apoptosis, police DNA damage, and respond to contact inhibition to prevent overcrowding (Sherr, 2004). Sarcomas and hematopoietic malignancies arise from the activation of oncogenes, while carcinomas result from the deactivation of tumor suppressors (Croce, 2008). The DNA mutation that occurs in both these gene types to activate or inactivate them can result from a variety of assaults. Ionizing radiation is known for its tendency to cause chromosomal translocations, leading to gene fusions. This can lead to formation of gene products with new function, or, if proto-oncogenes are fused to a strong promoter, upregulation of the gene (Mitelman et al., 2007). Chemical carcinogens such as tobacco smoke can cause cells to become cancerous, either through direct mutation of DNA, or promotion of proliferation of mutated cells (Irigaray and Belpomme, 2010). Certain types of viruses can introduce exogenous oncogenes, promote proliferation, or inhibit apoptosis, leading to malignancies (Dayaram and Marriott, 2008). Some mutations in oncogenes or tumor suppressors are inherited from the parents, leaving a person genetically susceptible to cancer (Robson and Offit, 2010). Whatever the cause, these mutations tend to facilitate

the accumulation of more mutation. For instance, mutations that occur in genes that code for DNA repair enzymes allow the cell to tolerate the buildup of further DNA mutations. Also, mutations that cause cells to proliferate quickly can cause failure in DNA repair, thereby increasing the speed at which more mutations accumulate. In this manner, cancer development is a multistep, gradual process that can display positive feedback in its ability to accelerate progression as it advances (Hanahan and Weinberg, 2000).

Differences Between Cancerous and Normal Cells

Accumulation of severe DNA damage causes cancer cells to differ markedly from the cell types from which they arise. The most notable difference is rapid and sustained proliferation. In order to grow, normal cells require stimulation by signals such as growth factors and extracellular matrix and cell-to-cell interactions. Cancer cells, however, are able to divide continually without these signals. This is accomplished by the production of growth factors that self-stimulate cancer cells to proliferate. An example of this is cancer cells that upregulate production of growth signals to which they respond, such as transforming growth factor alpha (TGF-α) (Hanahan and Weinberg, 2000). In addition, cancerous cells often have acquired immortality; they fail to lose replicative ability after an allotted number of doublings. The telomeres, or chromosome ends, of DNA contain a large but finite number of repeated sequences, which shorten each time the chromosome replicates. When this protective end is completely depleted, the affected cell dies (Counter et al., 1992). Cancer cells upregulate the telomerase enzyme responsible for adding those DNA repeat sequences and maintain their telomeres indefinitely (Bryan and Cech, 1999). In addition to stimulating their own growth in the absence of exogenous

signals, cancerous cells are capable of ignoring growth inhibition and pro-apoptotic signals. For instance, TGF-beta normally inhibits inactivation of the retinoblastoma protein (pRb), thereby blocking a pathway that leads to transition from the G1 stage of the cell cycle to the S phase. Many cancers have dysfunctional TGFB, which leads to their ability to ignore antiproliferative signaling through the pRb pathway (Hannon and Beach, 1994). Over 50% of all cancers are capable of ignoring apoptotic signals through the loss of function of the p53 protein, which induces apoptosis in cells in response to DNA abnormality; others can produce Insulin Like Growth Factor (IGF) survival signals (Levine, 1997; Evan and Littlewood, 1998). Cancerous cells often have gained the ability to stimulate angiogenesis, or blood vessel formation, to tumors. In fact, tumor size is highly limited until "angiogenic switch" occurs, where the tumor is able to acquire its own oxygen supply (Hanahan and Folkman, 1996). In many tumors, this is through an increased production of Vascular Endothelial Growth Factor (VEGF) and Fibroblast Growth Factor (FGF) (Hanahan and Folkman, 1996; Veikkola and Alitalo, 1999). Perhaps the most dangerous characteristic of cancer cells is their ability to invade surrounding tissues and metastasize to other sites in the body; in fact, 90% of cancer fatalities involve metastases (Sporn, 1996). When normal cells become densely packed into an area, they are signaled to stop dividing to prevent overgrowth. Cancer cells, however, are able to continue to divide and invade the surrounding tissues (Hanahan and Weinberg, 2000). One mechanism that allows for this in cancers of epithelial origin is through the loss of function of certain cell-cell interaction molecules. One such molecule is E-cadherin, which is expressed on the outer surface of cells. When two E-cadherins are bridged by contact between adjacent cells, growth in those cells is inhibited. A majority

of cancer cells of epithelial origin have lost E-cadherin, either through mutation or downregulation of expression (Christofori and Semb, 1999). Many mechanisms for metastases exist, but are exceedingly convoluted and presently poorly understood (Hanahan and Weinberg, 2000). Another very important feature of cancer is its higher rate of mutation from loss of DNA damage recognition and repair enzymes (Lengauer et al., 1998). Importantly, this can not only result in rapid accumulation of the traits described above, but also in resistance to anticancer drugs. This makes the ongoing discovery of new drugs of vital importance to cancer treatment.

Cancer Treatments in Use Today

Ionizing radiation is well known for its ability to damage DNA, which can lead to cancer. It can also, however, be used to damage the DNA locally in tumors, causing cell death. Most forms of radiation therapy actually work via induction of free radicals, which then damage the cancer cell's DNA (Tabassum et al., 2010). However, in hypoxic, or low oxygen tumor environments there can be 2 to 3 times more resistance to radiation therapy (Harrison et al., 2002). Side effects include damage to epithelium, swelling, fibrosis, or loss of elasticity in the area, hair loss, fatigue, and depression (Berkey, 2010). Importantly, another side effect of radiation therapy is secondary malignancy 20-30 years after treatment, though this is not common (Ural et al., 2007).

Existing chemotherapeutics attempt to inhibit the cellular functions that are most different between normal and cancerous cells such as cell division and DNA replication. While these metabolic processes occur more frequently in cancer cells, they also

commonly occur in normally dividing cells, leading to the potentially dangerous side effects associated with chemotherapy.

Alkylating agents include commonly known drugs such as Chlorambucil and work by adding alkyl groups to DNA, thereby crosslinking the strand. This DNA damage leads to the initiation of apoptosis, likely through p53, so cancers with alterations to this enzyme may have poor responses to these drugs (Begleiter et al., 1996). This group also includes the platinum complexes, such as Cisplatin and Carboplatin, which bind intra- or inter-strand guanine bases, also crosslinking DNA and triggering apoptosis (Bose, 2002). Cisplatin is also capable of forming protein-cisplatin complexes that inhibit glycolytic enzymes, thereby attacking cancer cell metabolism. This makes cisplatin effective against cancers of multiple origins, including cervical and lung cancer and lymphoma (Rodriguez-Enriquez et al., 2009). Antimetabolites act as analogs to the normal building blocks of DNA and RNA, and so block the incorporation of the natural purines and pyrimidines. This causes toxicity to cells attempting to replicate their DNA (Rodriguez-Enriquez et al., 2009). There also exist many natural products, which includes the Anthracyclines, Taxanes, and Vinca Alkaloids. Anthracyclines, such as Doxorubicin and Daunorubicin, act by inserting themselves into DNA, called intercalation, causing inhibition of the Topoisomerases-enzymes that assist in supercoiling the double helix, which are required for both DNA replication and division (Hershman and Shao, 2009; Masai et al., 2010). Vinca Alkaloids like Vincristine and Vinblastine bind tubulin and inhibit synthesis of the microtubules needed for mitosis. Taxanes such as Paclitaxel actually promote microtubule stability, which halts the cell in mitosis, eventually causing

apoptosis. Taxanes tend to suffer from high toxicity and susceptibility to drug resistance through the common drug efflux protein P-glycoprotein, making their use limited (Canta et al., 2009). Often, several drugs are used in combination to obtain maximum effect, but this may lead to an increase in unhealthy side effects (Peters et al., 2000). Common to all these drugs is their dramatic toxicity to cells that rapidly replicate. While many cells in the body are quiescent and so are less affected by chemotherapy, there are those that are dramatically affected, leading to side effects. Hematopoietic cells of the bone marrow rapidly divide and so a common toxicity associated with chemotherapy is bone marrow depression, which leads to anemia and immune suppression. Cells of the intestinal mucosa are also highly affected, causing nausea and vomiting in patients (Takimoto and Calles, 2009). These side effects combine to make the therapeutic index, or ratio of lethal to effective dose, of many chemotherapy drugs quite low (Bosanquet and Bell, 2004). For instance, Doxorubicin can interact with iron in the body to release reactive oxygen that causes cardiotoxicity, making its therapeutic index in vitro around ten (Hershman and Shao, 2009; Bosanquet and Bell, 2004).

Another class of drugs exist known as targeted molecular therapies, a highly diverse group of drugs that inhibit processes that may be important for cancer progression. For instance, Gefitinib inhibits signal transduction through the Epidermal Growth Factor Receptor (EGFR) by interfering with its effector receptor, tyrosine kinase (Takeuchi and Ito, 2010). Cetuximab is an antibody that directly binds the extracellular domain of the EGFR, preventing the binding of its ligand. Cetuximab can cause pulmonary toxicity and renal failure, and is very expensive at $30,000 per 8 weeks of

treatment (Bou-Assaly and Mukherji, 2010). Bevacizumab binds Vascular Endothelial Growth Factor (VEGF) and blocks interaction with its receptor, preventing angiogenesis to tumor sites. Inhibitors of VEGF, when used to treat lung cancers, can cause hemoptysis (bleeding in the lungs and airways), which occurred in one study in six of 66 individuals tested, four of them fatal (Peerzada et al., 2010). Tamoxifen antagonizes the estrogen receptor, causing death in breast cancers that are estrogen dependent, and can also inhibit other processes such as protein kinase C pathways, among others (de Medina et al., 2004). Though they are believed to be fairly well tolerated, these drugs also have side effects, and only tumor cells that have aberrancies in their target process will respond. Another problem with these drugs is their selection for mutations that render the cancer cells resistant to them, much of the time through a change in the binding site of the drug. Because cancer cells tend to tolerate mutations, their DNA can be highly mutable, leading to rapid development of resistance and resulting resurgence of malignancies (Hongbin, 2010). The unhealthy side effects of radiation, traditional chemical therapies, and targeted therapies, combined with increasing drug resistance, make the need for discovery of new, safe drugs both urgent and ongoing.

Nanotechnology Applications in Cancer Treatment

Nanomedicine, the use of nanotechnology in medical applications, has been greatly increasing in recent years. Research in the area of NP for imaging and drug delivery has become a major focus in cancer research. Many aspects of NP lend them utility in the destruction of cancer cells. The size of NP allows for them to gather in tumor sites, and their high surface reactivity can be exploited to attach additional

molecules to the surface. Nanoparticles are able to take advantage of the Enhanced Permeation and Retention (EPR) effect, which cause them to accumulate in tumors. Because tumors cause hurried angiogenesis to relieve low oxygen and nutrient conditions, leaky vasculature can result, with gaps between endothelial cells of 100 nm or more. This, combined with poor lymphatic drainage in tumors, can result in a passive buildup of NP in tumor sites (Cho et al., 2008). Some types of NP may be coated to help avoid rapid clearance of the drug by the reticuloendothelial system (Akerman et al., 2002). Nanoparticle surface reactivity allows for potential conjugation with biomolecules, which can be used for active targeting of cancer sites or for attachment of chemotherapeutics, enhancing their effects (Akerman et al., 2002).

Current Nano-Cancer Treatments

Nanotechnology has found a niche in recent years in oncology. As described above, many properties of NP make them useful, as well as adaptable in cancer treatment. The use of nanomaterials for imaging has been previously outlined, and their enhanced permeation and retention makes them ideal for imaging tumors (Nie et al., 2007). They can also be conjugated to targeting molecules that can label metastasizing cancer cells before clinical signs appear, improving the patient's prognosis (Mahmoud et al. 2010). Existing chemotherapies have also been improved using nanotechnology. For instance, a new drug Myocet uses doxorubicin incorporated into liposomes to retain its efficacy while ameliorating some of the side effects associated with doxorubicin such as cardiotoxicity (Batist et al., 2002). Another interesting area of research uses gold NPs to induce hyperthermia in tumors. Conjugation with Cetuximab, an antibody that targets

EGFR-expressing cancers, causes the NP to be internalized by malignant cells. Subsequent exposure to shortwave radiofrequency energy, which is highly penetrant and non-ionizing, heats the NP sufficiently to kill the tumor cells without harm to surrounding tissues (Cherukuri and Curley, 2010). Quantum dots are being investigated for their potential to kill cancer cells via photodestruction. Because quantum dots exhibit quantum confinement, stimulation with light energy can cause liberation of valence band electrons into the conduction band, which, in oxygenated environments, leads to generation of reactive oxygen species. Organic photodynamic therapies (PDT) exist, but suffer from a need to be excited by light in either the visible or UV spectrum, which cannot readily penetrate into tissues. It is believed that the use of nanomaterial quantum dots that show absorption in the near-infrared region will help to overcome tissue penetrance limitation (Samia et al., 2003). Conjugation with targeting molecules is also expected to improve the selectivity of photodestruction to tumor sites (Bakalova et al., 2004).

In summary, NP of many types through their novel physical, chemical, and quantum properties have demonstrated utility through various mechanisms against malignancies. In this study, we demonstrate the intrinsic ability of NP composed of ZnO to selectively kill certain types of cancerous cells. We also study the possible mechanisms of this selectivity from two angles: differences between cancerous and normal cells that may render them susceptible, including rapid proliferation rates, and NP characteristics that make them useful against cancer cells.

Cell Proliferation

Cell Cycle

Cells in the body must replicate in order for the organism to grow and develop, repair damaged tissue, and replace dying cells. All cells participate in at least certain components of a common set of phases known as the cell cycle. Those that do not replicate exit the normal cell cycle and enter a phase known as G_0, a resting state with respect to cell proliferation. While these cells do not divide, they continue to perform the function of the tissue in which they are found and can re-enter the cycle if stimulated (Smith and Martin, 1973). For instance, most highly differentiated cells such as neurons enter G_0 after the development of an organism is complete and are thereafter non-renewable (Liu et al., 2010). Cells that are proliferating, however, go through two distinct phases involved in cell division, interphase and mitosis. Interphase involves accumulation of elements needed for mitosis, which is division of the cell's DNA, and has three sub-phases (Nasmyth, 1996).

Gap 1, or G_1, involves growth and accumulation of cytoplasmic elements needed for DNA replication. A checkpoint exists before the cell leaves G_1 in which the DNA is assessed for damage and completeness before replication begins. This is highly regulated by the tumor suppressor protein p53, which halts the cell cycle and initiates DNA repair if damage is found, or signals apoptosis if damage cannot be repaired (Sherr, 1996). After this checkpoint, the cell enters the S, or synthesis phase, during which the DNA is replicated by the Polymerase enzyme. Replication is semi-conservative; as the double

helix of the DNA is unwound, each strand is used as a template to which Polymerase adds the complimentary bases. This process results in two daughter strands that contain one parent strand, and remain attached to one another at the centromere as sister chromatids until separation occurs during mitosis (Masai et al., 2010). Another gap phase follows, G_2, in which the cell continues growth and synthesizes microtubules required for mitosis. Another checkpoint exists at the close of G_2 to allow the cell to ensure that faithful replication of DNA has occurred to prevent the passage of incorrect genetic information to daughter cells. This assessment is performed by proofreading enzymes that are different than those in G_1, and interestingly, whose genes are rarely mutated in cancer. This is highly contrary to the G_1 checkpoint enzyme p53, which is the most common mutation seen in malignancies. If the checkpoint is passed, the cell will enter mitosis, or M phase (Kuntz and O' Connell, 2009).

Mitosis refers to the stage of the cell cycle in which the replicated DNA is divided. There are four phases of mitosis: Prophase, Metaphase, Anaphase, and Telophase. In Prophase, DNA condenses from loose chromatin into compact chromosomes. The mitotic spindle assembles at each centriole found on opposite poles of the nucleus, and microtubules attach to kinetochores on either side of the centromere of each chromosome (Hirano, 2005). The nuclear membrane degenerates to allow spatial separation of the divided DNA (Larijani and Poccia, 2009). During Metaphase, the chromosomes are lined up along the metaphase plate in the center of the cell, with microtubules extending out either side of the centromeres to the mitotic spindle (Rieder and Salmon, 1994). Anaphase is hallmarked by the breakdown of the proteins that attach

the sister chromatids, and the physical separation of them via shortening of the microtubules (Maiato and Lince-Faria, 2010; Guacci, 2007). During Telophase, two new nuclear membranes form, sequestering each separated set of chromosomes, and the DNA decondenses back into chromatin (Larijani and Poccia, 2009). The cell typically also begins cytokinesis, which is the separation of cytoplasm, to eventually form two distinct cells (Debec et al., 2010).

Microtubule Polymerization and Depolymerization

Microtubules are not only key players in cell motility and vesicle trafficking, they also are responsible for the movement and separation of chromosomes during mitosis (Maiato and Lince-Faria, 2010). They are hollow cylindrical polymers made up of subunits of α and β tubulin that form heterodimers. These subunits form long chains that complex laterally to form a long tube with one end of the cylinder having an exposed α subunit, and the other end containing an exposed β subunit. These are referred to as the minus end and plus end, respectively. Each subunit has a bound GTP molecule, which, when hydrolyzed to GDP, causes rapid depolymerization of the microtubule. However, most subunits that make up the polymer have bound GDP; GTP is typically only found on the microtubule ends. The GTP-binding site on the α subunit is relatively hidden, so its GTP is therefore hydrolyzed much more slowly than that on the β subunit, making the plus end the more dynamic of the two (Zheng, 2004). Stabilizing the dynamic end of the microtubule is accomplished by attaching a GTP-bound β subunit "cap" to the plus end to prevent depolymerization of the many GDP-bound subunits beneath it. Microtubule dynamics are accomplished in several ways: slow progressive hydrolysis and loss of

tubulin at the minus end, addition of subunits to the plus end, or hydrolysis and rapid loss of tubulin from the plus end, known as microtubule catastrophe (Risinger et al., 2009). These methods allow for purposeful treadmilling, lengthening, and shortening, known collectively as microtubule dynamics. Disrupting these dynamics can interfere with cellular processes such as mitosis, and can even arrest cell growth, as was discussed for certain chemotherapeutic drugs (Wilson et al., 1999).

Cell Synchronization and Inhibition of Proliferation

Often, cell proliferation needs to be inhibited or many cells need to be synchronized in a certain phase of the cell cycle. For instance, karyotypes are often observed to detect chromosomal abnormalities that put an individual at high risk for cancer. A karyotype is a spread of all of an individual's chromosomes that have been stained to improve visualization (Schrock et al., 1996). However, because individual chromosomes are only visible in a condensed state, the chemical Colcemid is used to arrest the cells in Metaphase of mitosis (Singh et al., 2001). There exist several chemical inhibitors that, through differing mechanisms of action, will synchronize cells in different phases of the cell cycle. These drugs are often used in molecular biology experiments for synchronization, or to simply slow proliferation of the cells. Two cell cycle inhibitors were used in this work: Nocodazole, and Colcemid. For these studies, we arrest proliferation using both chemical inhibitors and non-chemical methods to determine what effect, if any, proliferation had on cancer cell susceptibility to nanoparticle toxicity.

Aphidicolin is reported to arrest cells in early DNA synthesis phase via inhibition of DNA Polymerase (Spadari et al., 1985). Both Nocodazole and Colcemid have been shown to synchronize cells in mitosis through their interaction with microtubules. Colcemid works through two mechanisms: first, it binds with high affinity to unpolymerized heterodimers between the α and β subunits, lowering the ability of those heterodimers to incorporate into growing chains and thus slowing microtubule polymerization (Risinger et al., 2009). Secondly, colcemid can complex with polymerized end tubulin (though with lower affinity than soluble heterodimers) and cause a conformational change in the subunit that sterically inhibits lateral interactions between chains. This results in a "fraying" of the strands of tubulin that make up microtubules and subsequent depolymerization (Bhattacharyya et al., 2008). Nocodazole is capable of this same depolymerization via the disruption of interchain attachment, but also promotes hydrolysis of the "cap" GTP to GDP four to five-fold; because GDP-bound tubulin is unstable, rapid depolymerization occurs (Mejillano et al., 1996). A common, chemical-free method for proliferation reduction called serum deprivation was also used in this work. Culturing cells in media with lower serum concentration than normal for short periods (approximately 24 hours for this work) can cause them to enter a resting state without causing significant cell death (Kues et al., 2000). For this work, serum deprivation (2% FBS instead of standard 10%) was used in a T cell leukemic lineage to arrest cell growth. A variation of serum starvation, growth factor deprivation, was used in an epithelial cell line to the same end, which involes culturing in media lacking supplementation with Epidermal Growth Factor. Collectively, these chemical and non-

chemical methods were used in different cell types to assess the effect of rapid proliferation on susceptibility to nanoparticle cytotoxicity.

Reactive Oxygen Species

Reactive oxygen species (ROS) are molecules made up of or containing oxygen that have unpaired valence electrons, making them extremely reactive. These include superoxide ($\cdot O_2^-$), hydroxyl radicals ($\cdot OH$), and hydrogen peroxide (H_2O_2). Buildup of these can cause damage to membranes, proteins, and DNA, and lesions in tumor suppressor genes and proto-oncogenes can result in carcinogenesis (Zorov et al., 2005). ROS can be generated both exogenously and endogenously through natural cellular processes. Exogenous sources include ionizing radiation and UV light, and are often mutagenic (Higuchi, 2003). Endogenous production of ROS occurs via several natural mechanisms, such as during the breakdown of some chemicals by cytochrome p450 enzymes, and as a byproduct of cellular metabolism (Cederbaum et al., 2009). Reactive oxygen is used by cells during redox signaling, and its reactivity and toxicity is exploited by cells of the immune system to kill invading pathogens (Valko et al., 2007).

Metabolically generated ROS are those most relevant to this work, as the differential production between cancerous and normal cells may contribute to the selective cytotoxicity of ZnO NP to cancer cells. In order to survive, all cells must convert food energy, or sugars, into usable cellular energy in the form of adenosine triphosphate (ATP) (Nath, 2002). ATP contains adenosine, which is adenine bonded to a ribose, to which is attached a chain of three phosphate groups. Each ATP molecule contains two high-energy phosphate bonds (those between two phosphate groups), which

are used as energy currency for the cell (Boyer, 1989). Many energy-requiring cellular processes are coupled to the hydrolysis of ATP to ADP, harnessing the energy from the phosphate bond (Boyer, 1989). However, this requires that the cellular stores of ATP be replenished from ADP and inorganic phosphate (Nath, 2002). The process that accomplishes this is called cellular respiration, which is comprised of a series of steps including: glycolysis, pyruvate decarboxylation, the citric acid cycle, and oxidative phosphorylation (Pathania et al., 2009). It is during oxidative phosphorylation, specifically electron transport, where the majority of ATP is generated, that reactive oxygen is produced endogenously in cells during metabolic reactions (Nicholls, 2002). The electron transport chain involves a set of redox reactions in which electrons are shuttled through a series of protein carriers (Complex I – IV) in the mitochondrial inner membrane and finally to the terminal acceptor oxygen reducing it to water (Pathania et al., 2009). Coupled to this shuttling process is the transport of protons across the mitochondrial membrane. This produces a proton gradient, the equilibration of which provides the free energy to drive the phosphorylation of ADP to ATP by ATP synthase (Nicholls, 2002; Pathania et al., 2009). Superoxide is generated when an oxygen molecule is prematurely reduced by an electron carrier, which is believed to occur in approximately 2% of consumed oxygen atoms (Boveris and Chance 1973; Fridovich, 1995). This reactive oxygen is believed to be responsible for cellular aging (Nicholls, 2002).

Reactive oxygen molecules are highly damaging to cells; because of this, aerobic organisms have mechanisms through which they are neutralized to prevent toxicity. Superoxide dismutase catalyzes the conversion of superoxide to hydrogen peroxide and

oxygen. Catalase then converts hydrogen peroxide to water and molecular oxygen, and glutathione peroxidase catalyzes the reduction of hydrogen peroxide to water by glutathione (Chaudiere and Ferrari-Iliou, 1999). When insufficient levels of these enzymes or glutathione exist in a cell, or when these processes are overwhelmed by reactive oxygen assaults, a condition known as oxidative stress occurs. High levels of hydrogen peroxide build, which are then converted through the Fenton reaction to toxic hydroxyl radicals, which are capable of damaging nearly all biomolecules and for which no enzymatic neutralization reaction exists (Imlay, 2003). Interestingly, the Fenton reaction is catalyzed by free iron, which can be liberated from iron-sulfer clusters in enzymes by oxidative stress, increasing its availability to participate in hydroxyl radical formation (Fridovich, 1995). Also, the reactivity of hydroxyl radicals ensures that they will react with nearby biomolecules rather than diffuse across distances, and the ability of nucleic acids to bind iron make DNA a superior target of Fenton-created hydroxyl radicals (Fridovich, 1995). However, mitochondria are not only major producers of ROS; they are also the cellular targets of apoptosis induced by oxidative stress. Oxidative stress can trigger loss of mitochondrial membrane potential, which in turn increases electron "leak" and further generation of ROS, setting off a cascade that ultimately results in the opening of the mitochondrial permeability transition pore, and subsequent release of cytochrome C, which initiates apoptotic enzymes (Zamzami et al., 1995; Zorov et al., 2006). Necrotic cell death can also occur at extremely high levels of oxidative stress (Higuchi, 2003). Supplementation of cells with antioxidants can help alleviate this oxidative stress. For instance, N-Acetyl Cysteine (NAC) is a cell permeant glutathione precursor, which can be used to replenish the cellular stores of the molecule that donates

an electron to reactive oxygen, thereby neutralizing its reactivity (Chaudiere and Ferrari-Iliou, 1999; Sinha-Hikim et al., 2010). Cells maintain a delicate balance of reactive oxygen and antioxidant mechanisms; disruption of this balance by exogenous assaults leads to malignancy, apoptosis, and necrosis.

Studies have shown that malignant cells may be less tolerant of assaults by reactive oxygen due to higher intrinsic levels of oxidative stress. This elevated ROS results from an increased metabolic demand associated with rapid proliferation and greater mitochondrial dysfunction in cancer cells (Hileman et al., 2004; Pelicano et al., 2004). Interestingly, it has been found that oncogenes can induce ROS production in cells, and many human cancer lines show constitutive production of hydrogen peroxide (Vafa et al., 2002; Hlavata et al., 2003; Szatrowski and Nathan, 1991). While some malignant cells respond to this increased oxidative stress by elevating levels of antioxidant enzymes, this has limited capacity, and some cancer cells actually have reduced levels of superoxide dismutase (Hitchler et al., 2008; Oberley et al., 1978). In fact, one study showed that reduced superoxide dismutase was found in cancerous murine hepatocytes, but not those that were normal but rapidly proliferating during regeneration (Oberley et al., 1978). This demonstrates a weakness that can be exploited to selectively target malignant cells therapeutically without damaging normal cell types.

Cellular Uptake

An important facet of the study of the toxicity and medicinal efficacy of any substance is where it localizes and how it does so, both *in vivo* and cellularly. Studies from our lab thus far focus upon the cellular aspect of uptake and distribution. Certain

lipophilic drugs are able to passively diffuse across cell membranes, but many materials must be actively imported into cells, either through transport proteins or by endocytosis (Scherrmann, 2009). Endocytosis refers collectively to a group of different processes involving vesicle formation in the cell membrane that result in the internalization of substances as diverse as: pathogens, signaling molecules, proteins, extracellular fluid and dissolved substances, and particulate matter (Doherty and McMahon, 2009). Several endocytic pathways exist that are responsible for many functions, including regulating the cell surface topography with respect to receptors, pathogen internalization for destruction and antigen presentation, and nutrient uptake (Shroeder et al., 2010; Sorkin and von Zastrow, 2002). The most highly studied pathways are Clathrin-mediated, caveolae-mediated, and phagocytosis and macropinocytosis.

Clathrin-mediated endocytosis involves the import of pits or vesicles coated with the protein Clathrin. This pathway is characteristic of receptor-mediated endocytosis and is responsible for the internalization of G-protein couple receptors (GPCR) and receptor tyrosine kinases (RTK) (Sorkin and von Zastrow, 2002). Cell surface receptors involved in this type of import have adaptor proteins that, upon ligand binding to the receptor, recruit proteins important for changing the curvature of the plasma membrane. Epsin is responsible for the insertion of an amphipathic "wedge" into the membrane, which causes curvature, and clathrin forms lattices that stabilize the structure while Dynamin promotes closure of the invagination (Ford et al., 2002; McNiven et al., 2000). Once the Clathrin-coated pit is completely internalized, Auxilin and Hsc70 remove the Clathrin lattice before the endosome is trafficked to its destination (Eisenburg and Greene, 2007). An important feature of this endocytic pathway is its cargo specificity; adaptor proteins

ensure that only cargoes for which they have affinity will cause Clathrin recruitment and subsequent internalization (Doherty and McMahon, 2009).

Another method for cellular uptake involves Caveolae, or "mini caves" and is Caveolin-dependent. Caveolae are specialized lipid rafts that originate in the Golgi and form flask-like invaginations in the membrane (Tagawa et al., 2005). The protein Caveolin-1 has both its C and N-terminus on the cytosolic side, but inserts a hairpin structure into the membrane forming a curvature (Shlegel and Lisanti, 2000). This pathway is also cargo specific and is responsible for the import of some glycosylphospatidylinositol (GPI) anchored proteins, which are found concentrated in lipid rafts. Many other GPI-linked proteins are internalized through as yet not well understood mechanisms that are highly cholesterol dependent but do not require either Clathrin or Caveolae (Lakhan et al., 2009).

Certain cell types will perform a specialized type of endocytosis known as phagocytosis, or "cell eating," which involves the engulfment of large particles (usually over 0.5 microns) (May and Macheski, 2001). This is limited to cells such as monocytes, macrophages, dendritic cells, and neutrophils of the immune system. These cells are responsible for the removal of bacteria, dead cells, and apoptotic debris from the blood and tissues (Krauss, 2000). When pathogens and debris are found in the body, they are coated with opsonins, which may be either complement proteins or antibodies that cause clumping of particles together and facilitate phagocytosis. Professional phagocytes have receptors on their cell surface that recognize the Fc, or tail end, of antibodies and complement proteins. Interaction of these receptors with their ligands stimulates Actin remodeling and extension of the membrane around the particle to engulf it (May and

Macheski, 2001). This large internalized vesicle, the phagosome, fuses with lysosomes, where pathogens and debris are exposed to digestive enzymes, low pH, and often reactive oxygen such as hydrogen peroxide (Babior, 2000; Haas, 2007). This digestion can be followed by antigen processing and presentation to T cells of the immune system (Vyas et al., 2008).

Macropinocytosis is an important endocytic pathway that involves internalization of large volumes of extracellular fluid and the dissolved substances and particulate matter contained therein. During this process, large inward ruffles appear in the membrane, covering a large surface area of plasma membrane and encompassing large volumes of fluid, which can result in the non-specific uptake of any solid or dissolved matter in that liquid (Kerr and Teasdale, 2009). It is important to note that while phagocytosis and macropinocytosis are often referred to as Actin-dependent, this can be misleading. All forms of endocytosis require changes in the shape of the cell's Actin cytoskeleton, therefore all are Actin-dependent.

Endocytosis Inhibition

There exist many chemical inhibitors for each endocytic pathway, but it is important to note that experiments have shown nearly all of them to be capable of non-specific inhibition of other pathways. For instance, Chlorpromazine is used often in molecular biology experiments to selectively block Clathrin-mediated endocytosis through its ability to cause Clathrin and AP2, an accessory protein necessary for Clathrin lattice assembly, to leave the plasma membrane and surround endosomes instead (Wang et al., 1993). Studies have shown, however, that Chlorpromazine can also inhibit

phagocytosis and macropinocytosis, both by altering the fluidity of the plasma membrane and through interference with phospholipase C, which regulates Actin behavior (Elferink, 1979; Ivanov, 2008). Actin depolymerizers have long been used to inhibit macropinocytosis and phagocytosis, but it is now believed that these should be used as general inhibitors of all pathways (Ivanov, 2008).

One inhibitor that has shown fair specificity toward lipid raft-dependent endocytosis is the antibiotic Filipin. Contrary to many of the Caveolae-dependent inhibitors, which simply inhibit cholesterol synthesis, thereby making it unavailable to membranes and causing a fairly universal inhibition of endocytosis, Filipin causes cholesterol in lipid rafts to aggregate, sequestering it (Ivanov, 2008; Rodal et al., 1999). This has been shown to prevent lipid raft import, but does not affect Clathrin-dependent mechanisms or macropinocytosis (Ros-Baro et al., 2001; Monis et al., 2006).

One highly unselective endocytosis inhibitor was used in this work, Cytochalasin D, which works by depolymerizing F-actin. This prevents cytoskeletal rearrangements needed for the plasma membrane to change shape to accommodate internalization. This leads to a generalized inhibition of all pathways of endocytosis, including receptor-mediated, Caveolin-dependent, phagocytosis and macropinocytosis, along with the as yet not well characterized pathways that require morphological changes in the cell membrane (Ivanov, 2008).

Conclusion

In conclusion, the prevalence of nanomaterials in everyday products is on the rise, and with it the amount of human exposure to them. This necessitates a careful assessment

of NP interactions with biological systems and their toxicological properties. Oxidative stress has become the paradigm mechanism for toxicity, but further probing is necessary to understand the nature of this ROS generation, particularly if it may be useful to destroy undesired cell types. The toxicity of NP has been heavily assessed in many organisms and cell types, including human cancer cells that are often used for *in vitro* studies due to their ease of culture. The goal of this work is to assess the selective nature of this toxicity and to determine if cancer cells are universally more susceptible to NP-induced death than are normal human cells of corresponding lineage. We hypothesize that cancer cells that have greater rates of proliferation are under greater oxidative stress intrinsically, and will be killed more readily than are normal cells due to their inability to tolerate further reactive oxygen assaults. This work also evaluates properties of the NP that may be important for toxicity, the modification of which may enhance their usefulness in the field of cancer therapeutics.

These studies are presented in multiple chapters, Chapter 2 assesses NP toxicity in cancerous and normal T cells, along with basic mechanisms, and was published prior to the writing of this thesis. Chapter 3 extends these studies to include cells of epithelial origin and delves further into understanding properties of both ZnO NP and malignant cells themselves that are responsible for this selective toxicity. Chapter 4 ties together both studies to answer the major questions of the thesis and acts as a conclusion chapter.

References

Akerman, M.E., Chan, W.C.W., Laakkonen, P., Bhatia, S.N., and Ruoslahti, E. (2002). Nanocrystal targeting in vivo. Proc. Natl. Acad. Sci. USA. 99, 12617-12621.

Altekruse, S.F., Kosary, C.L., Krapcho, M., Neyman, N., Aminou, R., Waldron, W., Ruhl, J., Howlader, N., Tatalovich, Z., Cho, H., et al. (2010) SEER Cancer Statistics Review, 1975-2007, National Cancer Institute. Bethesda MD, Available at: http://www.seer.cancer.gov/csr/1975_2007/index.html [Accessed September 9, 2010].

Babior, B.M. (2000). Phagocytes and oxidative stress. Am. J. Med. 109, 33-44

Bakalova, R., Ohba, H., Zhelev, Z., Ishikawa, M., and Baba, Y. (2004). Quantum dots as photosynthesizers? Nat. Biotechnol. 22, 1360-1361.

Batist, G., Barton, J., Chaikin, P., Swenson, C., and Welles, L. (2002). Myocet (liposome-encapsulated doxorubicin citrate): a new approach in breast cancer therapy. Expert Opin. Pharmacother. 3, 1739-1751.

Begleiter, A., Mowat, M., Israels, L.G., and Johnson, J.B. (1996). Chlorambucil in chronic lymphocytic leukemia: mechanism of action. Leuk. Lymphoma 23, 187-201.

Berkey, F.J. (2010). Managing the Adverse Effects of Radiation Therapy. Am. Fam. Physician 82, 381-388.

Bhattacharyya, B., Panda, D., Gupta, S., and Banerjee, M. (2008). Anti-Mitotic Activity of Colchicine and the Structural Basis for its Interaction with Tubulin. Med. Res. Rev. 28, 155-83.

Blank, V., Popov, M., and Pivovarov, G. (1998). Ultrahard and superhard phases of fullerite C60: comparison with diamond on hardness and wear. Diamond Related Materials 7, 427-431.

Bosanquet, A.G. and Bell, P.B. (2004). Ex vivo therapeutic index by drug sensitivity assay using fresh human normal and tumor cells. J. Exp. Therap. Oncol. 4, 145-154.

Bose, R.N. (2002). Biomolecular Targets for Platinum Antitumor Drugs. Mini Rev. Med. Chem. 2, 103-111.

Bou-Assaly, W. and Mukherji, S. (2010). Cetuximab (Erbitux). Am. J. Neuroradiol. 31, 626-627.

Boveris, A. and Chance, B. (1973). The mitochondrial generation of hydrogen peroxide. General properties and effect of hyperbaric oxygen. Biochem. J. 134, 707-716.

Boyer, P.D. (1989). A perspective of the binding change mechanism for ATP synthesis. FASEB J. 3, 2164-2178.

Bryan T.M. and Cech T.R.. (1999). Telomerase and the maintenance of chromosome ends. Curr. Opin. Cell Biol. 11, 318-324.

Canta, A., Chiorazzi, A., and Cavaletti, G. (2009). Tubulin: A Target for Antineoplastic Drugs into the Cancer Cells but also the Peripheral Nervous System. Curr. Med. Chem. 16, 1315-1324.

Cederbaum, A.I., Lu Y., and Wu, D. (2009). Role of oxidative stress in alcohol-induced liver injury. Arch.Toxicol. 83, 519-548.

Chaudiere, J. and Ferrari-Iliou, R. (1999). Intracellular Antioxidants: from Chemical to Biochemical Mechanisms. Food Chem. Toxicol. 37, 949-962.

Cherukuri, P. and Curley, S.A. (2010). Use of nanoparticles for targeted, noninvasive thermal destruction of malignant cells. Methods Mol. Biol. 624, 359-373.

Cho, K., Wang, X., Nie, S., Chen, Z.G., and Shin, D.M. (2008). Therapeutic nanoparticles for drug delivery in cancer. Clin. Cancer Res. 14, 1310-1316.

Christofori, G. and Semb, H. (1999). The role of cell-adhesion molecule E-cadherin as a tumour-suppressor gene. Trends Biochem. Sci. 24, 73-76.

Counter, C.M., Avilion, A.A., Lefeuvre, C.E., Stewar t, N.G., Greider, C.W., Harley, C.B., and Bacchetti, S. (1992). Telomere shortening associated with chromosome instability is arrested in immortal cells which express telomerase activity. EMBO J. 11, 1921-1929.

Croce, C.M., M.D. (2008). Oncogenes and Cancer. N. Engl. J. Med. 358, 502-511.

Dayaram, T. and Marriott, S. (2008). Effect of Transforming Viruses on Molecular Mechanisms Associated with Cancer. J. Cell. Physiol. 216, 309-314.

de Francisco, A. and Matlin, S.A. (2006). Monitoring Financial Flows for Health Research 2006: The changing landscape of health research for development. Global Forum for Health Research. Available at: http://www.globalforumhealth.org/Media-Publications/Publications/Monitoring-Financial-Flows-for-Health-Research-2006-The-changing-landscape-of-health-research-for-development. [Accessed January 16, 2010].

de Medina P., Favre, G., and Poirot, M. (2004). Multiple targeting by the antitumor drug tamoxifen: a structure-activity study. Curr. Med. Chem. Anticancer Agents 4, 491-508.

Debec, A., Sullivan, W., and Bettancourt-Dias, M. (2010). Centrioles: active players or passengers during mitosis? Cell. Mol. Life Sci. 67, 2173-2194.

Doherty, G.J. and McMahon, H.T. (2009). Mechanisms of Endocytosis. Annu. Rev. Biochem. 78, 857-902.

Eisenburg, E. and Greene L.E. (2007). Multiple roles of auxilin and hsc70 in clathrin-mediated endocytosis. Traffic 8, 640-646.

Elferink, J.G. (1979). Chlorpromazine inhibits phagocytosis and exocytosis in rabbit polymorphonuclear leukocytes. Biochem.Pharmacol. 28, 965-968.

Evan, G. and Littlewood, T. (1998). A matter of life and cell death. Science 281, 1317-1322.

Feynman, R. 1960. There's Plenty of Room at the Bottom. Caltech. Engineering and Science. Available at: http://www.zyvex.com/nanotech/feynman.html. [Accessed September 16, 2010].

Ford, M.G., Mills, I.G., Peter, B.J., Vallis, Y., Praefcke, G.J., Evans, P.R., and McMahon, H.T. (2002). Curvature of clathrin-coated pits driven by epsin. Nature 419, 361-366.

Fridovich, I. (1995). Superoxide Radical and Superoxide Dismutases. Annu. Rev. Biochem. 64, 97-112.

Generally Recognized as Safe. US Food and Drug Administration. 2009. Available at:http://www.fda.gov/Food/FoodIngredientsPackaging/GenerallyRecognizedasSafeGRAS/default.htm [Accessed September 6, 2010].

Greenberg, E., Divertie, M.B., and Woolner, L.B. (1964). A Review of Unusual Systemic Manifestations Associated with Carcinoma. Am. J. Med. 36, 106-120.

Guacci, V. (2007). Sister chromatid cohesion: the cohesion cleavage model does not ring true. Genes Cells 12, 693-708.

Haas, A. (2007). The phagosome: compartment with a license to kill. Traffic 8, 311-330.

Hanahan, D. and Folkman, J. (1996). Patterns and emerging mechanisms of the angiogenic switch during tumorigenesis. Cell 86, 353-364.

Hanahan, D. and Weinberg, R. (2000). The Hallmarks of Cancer. Cell 100, 57-70.

Hannon, G.J., and Beach, D. (1994). P15INK4B is a potential effector of TGF-beta-induced cell cycle arrest. Nature 371, 257-261

Harrison, L.B., Chadha, M., Hill, R., Hu, K., and Shasha, D. (2002). Impact of Tumor Hypoxia and Anemia on Radiation Therapy Outcomes. Oncologist 7, 492-508.

Hershman, D.L., M.D. and Shao, T., M.D. (2009). Antracycline Cardiotoxicity After Breast Cancer Treatment. Oncology 23, 227-234.

Higuchi, Y. (2003). Chromosomal DNA fragmentation in apoptosis and necrosis induced by oxidative stress. Biochem.l Pharmacol. 66, 1527-1535.

Hileman, E.O., Liu, J., and Albitar, M. (2004). Intrinsic oxidative stress in cancer cells: a biochemical basis for therapeutic selectivity. Cancer Chemother. Pharmacol. 53, 209-219.

Hirano, T. (2005). Condensins: organizing and segregating the genome. Curr. Biol. 15, R265-R275.

Hitchler, M.J., Oberley, L.W., and Domann, F.E. (2008). Epigenetic silencing of SOD2 by histone modifications in human breast cancer cells. Free Radic. Biol.Med. 45, 1573-1580.

Hlavata, L., Aguilaniu, H., and Pichova, A. (2003). The oncogenic RAS2(val19) mutation locks respiration, independently of PKA, in a mode prone to generate ROS. EMBO J. 22, 3337-3345.

Hoffman, A.J., Carraway, E.R., and Hoffman, M.R. (1994). Photocatalytic Production of H2O2 and Organic Peroxides on Quantum-Sized Semiconductor Colloids. Environ. Sci. Technol. 28, 776-785.

Hongbin, J. (2010). Mechanistic insights into acquired drug resistance in epidermal growth factor receptor mutation-targeted lung cancer therapy. Cancer Sci. 101, 1933-1938.

Imlay, J.A. (2003). Pathways of Oxidative Damage. Annu. Rev. Microbiol. 57, 395-418.

Irigaray, P. and Belpomme, D. (2010). Basic properties and molecular mechanisms of exogenous chemical carcinogens. Carcinogenesis 31, 135-148.

Ivanov, A.I. (2008). Pharmacological inhibition of endocytic pathways: is it specific enough to be useful? Methods Mol. Biol. 440, 15-33.

Jain, S., Xu, R., Prieto, V.G., and Lee, P. (2010). Molecular classification of soft tissue sarcoma and its clinical applications. Int. J. Clin.Exp. Pathol. 3, 416-429.

Jiang, W., Mashayekhi, H., and Xing, B. (2009). Bacterial toxicity comparison between nano- and micro-scaled oxide particles. Environ. Pollut. 157, 1619-1625.

Kaasgaard, T. and Adresen, T.L. (2010). Liposomal cancer therapy: exploiting tumor characteristics. Expert Opin. Drug Deliv. 7, 225-243.

Kerr, M.C. and Teasdale, R.D. (2009). Defining Macropinocytosis. Traffic 10, 364-371.

Krauss, K.H. (2000). Professional phagocytes: predators and prey of microorganisms. Schweizerische Medizinische Wochenschrift 130, 97-100.

Kues, W.A., Anger, M., Carnwath, J.W., Paul, D., Motlik, J., and Niemann, H. (2000). Cell Cycle Synchronization of Porcine Fetal Fibroblasts : Effects of Serum Deprivation and Reversible Cell Cycle Inhibitors. Biol. Reprod. 62, 412-419.

Kuntz, K. and O'Connell, M.J. (2009). The G(2) DNA damage checkpoint: could this ancient regulator be the Achilles heel of cancer? Cancer Biol. Ther. 8, 1433-439.

Lacerda, L., Bianco, A., Prato, M., and Kostarelos, K. (2006). Carbon nanotubes as nanomedicines: From toxicology to pharmacology. Adv. Drug Deliv. Rev. 58, 1460-1470.

Lakhan, S.E., Sabharanjak, S., and De, A. (2009). Endocytosis of glycosylphosphatidylinositol-anchored proteins. J. Biomed. Sci. 16, 93-104.

Larijani, B. and Poccia, D.L. (2009). Nuclear Membrane Formation: Mind the Gaps. Annu. Rev. Biophys. 38, 107-124.

Lengauer, C., Kinzler, K.W., and Vogelstein, B. (1998). Genetic instabilities in human cancers. Nature 296, 643-649.

Leukemia and Lymphoma Society. Disease Information. Available at: http://www.leukemia-lymphoma.org/all_page?item_id=7026. [Accessed September 16, 2010].

Levine, A.J. (1997). P53, the cellular gatekeeper for growth and division. Cell 88, 323-331.

Liu, D.Z., Ander, B.P., and Sharp, F.R. (2010). Cell cycle inhibition without disruption of neurogenesis is a strategy for treatment of central nervous system diseases. Neurobiol. Dis. 37, 549-557.

Mahmoud, W., Sukhanova, A., Oleinikov, V., Rakovich, Y.P., Donegan, J.F., Pluot, M., Cohen, J.H., Volkov, Y., and Nabiev, I. (2010). Emerging applications of fluorescent nanocrystals quantum dots for micrometastases detection. Proteomics 10, 700-716.

Maiato, H. and Lince-Faria, M. (2010). The perpetual movements of anaphase. Cell. Mol. Life Sci. 67, 2251-2269.

Mansur, H.S. (2010). Quantum dots and nanocomposites. Wiley Interdiscip. Rev. Nanomed. Nanobiotechnol. 2, 113-129.

Masai, H., Matsumoto, S., You, Z., Yoshizawa-Sugata, N., and Oda, M. (2010). Eukaryotic chromosome DNA replication: where, when and how? Annu. Rev. Biochem. 79, 89-130.

Material Safety Data Sheet: Zinc Oxide. Sigma Aldrich. Available at: http://www.sigmaaldrich.com/MSDS/MSDS/DisplayMSDSPage.do [Accessed September 6, 2010].

May, R.C. and Macheski, L.M. (2001). Phagocytosis and the actin cytoskeleton. J. Cell Sci. 114, 1061-1077.

McNeil, S.E. (2005). Nanotechnology for the biologist. J. Leukoc. Biol. 78, 585-594.

McNiven, M.A., Cao, H., Pitts, K.R., and Yoon, Y. (2000). The dynamin family of mechanoenzymes: pinching in new places. Trends Biochem. Sci. 25, 115-120.

Medintz, I.L., Uyeda, H.T., Goldman, E.R., and Mattoussi, H. (2005). Quantum dot bioconjugates for imaging, labeling and sensing. Nature Mat. 4, 435-446.

Mejillano, M.R., Shivanna, B.D., and Himes, R.H. (1996). Studies on the Nocodazole-Induced GTPase Activity of Tubulin. Arch Biochem Biophys 336, 130-138.

Mitelman, F., Johansson, B., and Mertens, F. (2007). The impact of translocations and gene fusions on cancer causation. Nat. Rev. Cancer 7, 233-245.

Monis, G.M., Schultz, C., and Ren, R. (2006). Role of endocytic inhibitory drugs on internalization of amyloidogenic light chains by cardiac fibroblasts. Am. J. Pathol. 169, 1939-1952.

Nath, S. (2002). The molecular mechanism of ATP synthesis by F1F0 ATP synthase: a scrutiny of the major possibilities. Adv. Biochem. Eng. Biotechnol. 74, 65-98.

National Cancer Institute. Costs of Cancer Care. Reviewed April 15, 2010. Available at: http://progressreport.cancer.gov/doc_detail.asp?pid=1&did=2007&chid=75&coid=726&mid=. [Accessed September 9, 2010].

National Cancer Institute. Cancer Research Funding. Reviewed July 13, 2010. Available at : http://www.cancer.gov/cancertopics/factsheet/NCI/research-funding. [Accessed September 9, 2010].

National Cancer Institute. What You Need to Know About Cancer. 2006. Available at http://www.cancer.gov/cancertopics/wyntk/cancer/page6. [Accessed September 9, 2010].

Nasmyth, K. (1996). Viewpoint: putting the cell cycle in order. Science 274, 1643-1645.

Nel, A., Xia. T., Madler, L., and Li, N. (2006). Toxic potential of materials at the nanolevel. Science 311, 622-627.

Nicholls, D.G. (2002). Mitochondrial function and dysfunction in the cell: its relevance to aging and aging-related disease. Int. J. Biochem. Cell Biol. 34, 1372-1381.

Nie, S., Xing, Y., Kim, G.J., and Simons, J.W. (2007). Nanotechnology applications in cancer. Annu. Rev. Biomed. Eng. 9, 257-288.

Oberley, L.W., Bize, I.B., Sahu, S.K., Leuthauser, S.W., and Gruber, H.E. (1978). Superoxide dismutase activity of normal murine liver, regenerating liver, and H6 hepatoma. J.Natl. Cancer Inst. 61, 375-379.

Pathania, D., Millard, M., and Neamati, N. (2009). Opportunities in discovery and delivery of anticancer drugs targeting mitochondria and cancer cell metabolism. Adv. Drug Deliv. Rev. 61, 1250-1275.

Plank, C., Schillinger, U., Scherer, F., Bergemann, C., Remy, J.S., Krotz, F., Anton, M., Lausier, J., and Rosenecker, J. (2003) The Magnetofection Method: Using Magnetic force to Enhance Gene Delivery. Biol. Chem. 384, 737-747.

Peerzada, M.M., Spiro, T.P., and Daw, H.A. (2010). Pulmonary toxicities of biologics: a review. Anticancer Drugs 21, 131-139.

Pelicano, H., Carney, D., and Huang, P. (2004). ROS stress in cancer cells and therapeutic implications. Drug Resist. Updat. 7, 97-110.

Peters, G.J., van der Wilt, C.L., van Moorsel, C.J.A., Kroep, J.R., Bergman, A.M., and Ackland, S.P. (2000). Basis for effective combination cancer chemotherapy with antimetabolites. Pharmacol. Ther. 87, 227-253.

Project on Emerging Nanotechnologies. (2010). Available at: http://www.nanotechproject.org/inventories/consumer/analysis_draft/, [Accessed September 1, 2010].

Reddy, K.M., Feris, K., Bell, J., Wingett, D.G., Hanley, C., Punnoose, A. (2007). Selective toxicity of zinc oxide nanoparticles to prokaryotic and eukaryotic systems. Appl. Phys. Lett. 90, 2139021-2139023.

Rhim, J.S. (1988). Viruses, Oncogenes, and Cancer. Cancer Detection and Prevention 11, 139-149.

Rieder, C.L. and Salmon, E.D. (1994). Motile kinetochores and polar ejection forces dictate chromosome position on the vertebrate mitotic spindle. J. Cell Biol. 124, 223-233

Risinger, A.L., Giles, F.J., and Mooberry, S.L. (2009). Microtubule Dynamics as a Target in Oncology. Cancer Treat. Rev. 35, 255-261.

Robson, M. and Offit, K. (2010). Inherited Predisposition to Cancer: Introduction and Overview. Hematol. Oncol. Clin. North Am. 24, 793-797.

Rodal, S.K., Skretting, G., Garred, O., Vilhardt, F., van Deurs, B., and Sandvig, K. (1999). Extraction of cholesterol with methyl-beta-cyclodextrin perturbs formation of clathrin-coated endocytic vesicles. Mol. Biol. Cell 10, 961-974.

Rodriguez-Enriquez, S., Marin-Hernandez, A., Gallardo-Perez, J.C., Carreno-Fuentes, L., and Moreno-Sanchez, R. (2009). Targeting of cancer energy metabolism. Mol. Nutr. Food Res. 53, 29-48.

Roomi, M.W., Monterrey, J.C., Kalinovsky, T., Rath, M., and Niedzwiecki, A. (2009). Distinct patterns of matrix metalloproteinase-2 and -9 expression in normal human cell lines. Oncol. Rep. 21, 821-826.

Ros-Baro, A., Lopez-Iglesias, C., and Peiro, S. (2001). Lipid rafts are required for GLUT4 internalization in adipose cells. Proc. Natl. Acad. Sci. USA 98, 12050-12055.

Saito, N., Usui, Y., Aoki, K., Narita, N., Shimizu, M., Hara, K., Ogiwara, N., Nakamura, K., Ishigaki, N., Kato, H., et al. (2009). Carbon nanotubes: biomaterial applications. Chem. Soc. Rev. 38, 1897-1903.

Samia, A.C.S., Chen, X., and Burda, C. (2003). Semiconductor Quantum Qots for Photodynamic Therapy. J. Am. Chem. Soc. 125, 15736-15737.

Scherrmann, Jean-Michele. (2009). Transporters in Absorption, Distribution, and Elimination. Chem. Biodivers. 6, 1933-1942.

Shlegel, A. and Lisanti, M.P. (2000). A molecular dissection of caveolin-1 membrane attachment and oligomerization. Two separate regions of caveolin-1 C-terminal domain mediate membrane binding and oligomer/oligomer interactions in vivo. J. Biol. Chem. 275, 21605-21617.

Schrand, A.M., Rahman, M.F., Hussain, S.M., Schlager, J.J., Smith, D.A., and Syed, A.F. (2010). Metal-based nanoparticles and their toxicity assessment. Wiley Interdiscip. Rev. Nanomed. Nanobiotechnol. 2, 544-568.

Schrock, E., Du Manoir, S., Veldman, T., Schoell, B., Wienberg, J., Ferguson-Smith, M.A., Ning, Y., Ledbetter, D.H., Bar-Am, I., Soenksen, D., et al. (1996). Multicolour Spectral Karyotyping of Human Chromosomes. Science 273, 494-497.

Sharma, S.K., Pujari, P.K., Sudarshan, K., Dutta, D., Mahapatra, M., Godbole, S.V., Jayakumar, O.D., Tyagi, A.K. (2009). Positron annihilation studies in ZnO nanoparticles. Solid State Commun. 149, 550-554.

Sherr, C. (1996). Cancer cell cycles. Science 274, 1673-1678.

Sherr, C.J. (2004). Principles of Tumor Suppression. Cell 116, 235-246.

Shroeder, F., Huang, H., McIntosh, A.L., Atshaves, B.P., Martin, G.G., and Kier, A.B. (2010). Calveolin, sterol carrier protein-2, membrane cholesterol-rich microdomains and intracellular cholesterol trafficking. Subcell. Biochem. 51, 279-318.

Sinha-Hikim, I., Shen, R., Paul, L.W.N., Crum, A., Vaziri, N.D., and Noris, K.C. (2010). Effects of a novel cystine-based glutathione precursor on oxidative stress in vascular smooth cells. American Journal of Physiology. Cell Physiol. 299, C638-C642.

Singh, B., Gogineni, S., Goberdhan, A., Sacks, P., Shaha, A., Shah, J., and Rao, P. (2001). Spectral karyotyping analysis of head and neck squamous cell carcinoma. Laryngoscope 111, 1545-1550.

Smith, J.A. and Martin, L. (1973). Do cells cycle? Proc. Natl. Acad. Sci. USA 70, 1263-1267.

Sorkin, A. and von Zastrow, M. (2002). Signal Transduction and Endocytosis: Close Encounters of Many Kinds. Nat. Rev. Mol. Cell Biol. 3, 600-614.

Sozer, N. and Kokini, J.L. (2009). Nanotechnology and its applications in the food sector. Trends Biotechnol. 27, 82-89.

Spadari, S., Focher, F., Sala, F., Ciarrocchi, G., Koch, G., Falaschi, A., and Pedrali-Noy, G. (1985). Control of cell division by aphidicolin without adverse effects upon resting cells. Arzneimittel-Forschung 35, 1108-1116.

Sporn, M.B. (1996). The war on cancer. Lancet 347, 1377-1381.

Sun, C., Lee, J.S.H., and Zhang, M. (2008). Magnetic nanoparticles in MR imaging and drug delivery. Adv. Drug Deliv. Rev. 60. 1252-1265.

Szatrowski, T.P. and Nathan, C.F. (1991). Production of large amounts of hydrogen peroxide by human tumor cells. Cancer Res. 51, 794-798.

Tabassum, A., Bristow, R.G., and Venkateswaran, V. (2010). Ingestion of selenium and other antioxidants during prostate cancer radiotherapy: A good thing? Cancer Treat. Rev. 36, 230-234.

Tagawa, A., Mezzacasa, A., and Hayer, A. (2005). Assembly and trafficking of caveolar domains in the cell: caveolae as stable, cargo-triggered, vesicular transporters. J. Cell Biol. 170, 769-779.

Takeuchi, K., and Ito, F. (2010). EGF receptor in relation to tumor development: molecular basis of responsiveness of cancer cells to EGFR-targeting tyrosine kinase inhibitors. FEBS J. 277, 316-326.

Takimoto, C.H., MD, PhD and Calles, A., MD. (2009). Chemotherapeutic agents and their usage, dosage and toxicities. Cancer Management: A Multidisciplinary Approach 11th Ed. Available at: http://www.cancernetwork.com/cancer-management-12/appendix4/article/10165/1406591. [Retrieved 16 September 2010] Electronic Citation

Ural, A.U., Beyzadeoglu, M., Avcu, F., and Nevruz, O. (2007). Chronic myeloid leukemia following radiotherapy for carcinoma of the cervix: report of a case and brief review of the literature. Am. J. Hematol. 82, 416-416.

Vafa, O., Wade, M., and Kern, S. (2002). C-Myc can induce DNA damage, increase reactive oxygen species, and mitigate p53 function: a mechanism for oncogene-induced genetic instability. Mol. Cell 9, 1031-1044.

Valko, M., Leibfritz, D., Moncol, J., Cronin, M.T., Mazur, M., and Telser, J. (2007). Free radicals and antioxidants in normal physiological functions and human disease. Int. J. Biochem. Cell Biol. 39, 44-84.

Veikkola, T. and Alitalo, K. (1999). VEGFs, receptors and angiogenesis. Semin. Cancer Biol. 9, 211-220.

Vyas, J.M., Van der Veen, A.G., and Ploegh, H.L. (2008). The known unknowns of antigen processing and presentation. Nat. Rev. Immunol. 8, 607-618.

Wang, L.H., Rothberg, K.G., and Anderson, R.G. (1993). Mis-assembly of clathrin lattices on endosomes reveals a regulatory switch for coated pit formation. J. Cell Biol. 123, 1107-1117.

Wilson, L., Panda, D., and Jordan, M.A. (1999). Modulation of microtubule dynamics by drugs: a paradigm for the actions of cellular regulators. Cell Struct. Funct. 24, 329-335.

World Health Organization. Cancer. Available at: http://www.who.int/mediacentre/factsheets/fs297/en/index.html [Accessed January 16, 2010].

Xia, T., Kovovich, M., and Liong, M. (2008). Comparison of the Mechanism of Toxicity of Zinc Oxide and Cerium Oxide Nanoparticles Based on Dissolution and Oxidative Stress Properties. ACS Nano 2, 2121-2134.

Xiang, S.D., Selomulya, C., Ho, J., Apostolopoulos, V., and Plebanski, M. (2010). Delivery of DNA vaccines: an overview on the use of biodegradable polymeric and magnetic nanoparticles. Wiley Interdiscip. Rev. Nanomed. Nanobiotechnol. 2, 205-218.

Yang, H., Liu, C., Yang, D., Zhang, H., and Xi, Z. (2009). Comparative study of cytotoxicity, oxidative stress and genotoxicity induced by four typical nanomaterials: the rold of particle size, shape and composition. J. Appl. Toxicol. 29, 69-78.

Zamzami, N., Marchetti, P., Castedo, M., Decaudin, D., Macho, A., Hirsch, T., Susin, S.A., Petit, P.X., Mignotte, B., and Kroemer, G. (1995). Sequential reduction of mitochondrial transmembrane potential and generation of reactive oxygen species in early programmed cell death. J. Exp. Med. 182, 367-377.

Zheng, Y. (2004). G Protein Control of Microtubule Assembly. Annu. Rev. Cell Dev. Biol. 20, 867-894.

Zorov, D.B., Bannikova, S.Y., Belousov, V.V., Vyssokikh, M.Y., Zorova, L.D., Isaev, N.K., Krasnikov, B.F., and Plotnikov, E.Y. (2005). Reactive oxygen and nitrogen species: friends or foes? Biochemistry 70, 215-21.

Zorov, D.B., Juhaszova, M., Sollot, S.J. (2006). Mitochondrial ROS-induced ROS release: An update and review. Biochim. Biophys. Acta 1757, 509-517.

CHAPTER 2: PREFERENTIAL KILLING OF CANCEROUS T CELLS BY ZINC OXIDE NANOPARTICLES

Introduction

The integration of nanotechnology and biology provides the opportunity for the development of new materials in the nanometer size range that can be applied to many potential applications in biological science and clinical medicine (McNeil, 2005; Lanone and Boczkowski, 2006; Groneberg et al., 2006). When reduced to the nanoscale realm, unique size-dependent properties of nanomaterials, including nanoparticles (NP), are manifested (Nel et al., 2006). One of the principal factors believed to cause properties of nanomaterials to differ from their bulk counterparts includes an increase in relative surface area and quantum effects, which can affect chemical reactivity and other physical and chemical properties (Lanone and Boczkowski, 2006; Nel et al., 2006). For example, a particle of 30 nm size has 5% of its atoms on its surface compared to 50% of the atoms on the surface of a 3 nm particle (Groneberg et al., 2006). The altered properties of NP, and their similarity in size compared to naturally occurring biological structures, can allow them to readily interact with biomolecules on both the cell surface and within the cell and potentially affect cellular responses in a dynamic and selective manner. Materials that exploit these characteristics are becoming increasingly attractive for use in novel biomedical applications.

Although our understanding of the functioning of the human body at the molecular and nanometer scale has improved tremendously, advances in therapeutic options for treating severe and debilitating diseases such as cancer and autoimmunity have lagged by comparison. In this regard, nanomedicine, which is the application of nanotechnology to medical problems, can offer new approaches. With regards to cancer treatment, most current anticancer regimes do not effectively differentiate between cancerous and normal cells. This indiscriminate action frequently leads to systemic toxicity and debilitating adverse effects in normal body tissues, including bone marrow suppression, neurotoxicity, and cardiomyopathy (Nie et al., 2007; Bosanquet and Bell, 2004). Nanotechnology and nanomedicine can offer a more targeted approach that promises significant improvements in the treatment of cancer (Nie et al., 2007). In this study, we have employed 8 nm zinc oxide (ZnO) NP in which the synthesis and properties have been previously described (Reddy et al., 2007). The aim of the study was to investigate whether ZnO NP induce toxicity in a cell-specific manner, determine the mechanism(s) of toxicity, and whether these NP have potential utility in novel biomedical applications seeking to eliminate pathogenic cells while sparing healthy body tissues.

Materials and Methods

Preparation and Characterization of Zinc Oxide Nanoparticles

ZnO NP were synthesized in diethylene glycol (DEG) by forced hydrolysis of zinc acetate at 160˚ C as previously described and size control achieved by optimizing the hydrolysis ratio (Reddy et al., 2007). The ZnO NP were separated from DEG via

centrifugation (15,000 rpm), washed with ethanol several times, and dried to obtain a nanoscale powder sample. The ZnO chemical phase, crystallite size (8-13 nm), and shape were confirmed using x-ray diffraction (XRD), transmission electron microscopy (TEM), and spectrophotometry (Reddy et al., 2007). The NP were then reconstituted in phosphate buffered saline (PBS) solution. After reconstitution, NP were sonicated for 10 min and immediately vortexed before addition to cell cultures.

Isolation of $CD4^+$ T Lymphocytes and Cell Culture

Written, informed consent was obtained from all blood donors and the University Institutional Review Board approved the study. Peripheral blood mononuclear cells (PBMC) were obtained by Ficoll-Hypaque (Histopaque-1077, Sigma, St. Louis, MO) gradient centrifugation using heparinized phlebotomy samples (Coligan, 1995). Cells were washed 3 times with Hank's buffer (Sigma) and incubated at 1×10^6 cells/mL in RPMI-1640 (Sigma) containing 10% fetal bovine serum (FBS). $CD4^+$ cells were obtained by negative immunomagnetic selection per manufacturer's instructions using a cocktail of antibodies against CD45RO, CD8, CD19, CD14, CD16, CD56, CD8, and glycophorin A (StemCell Technologies, Vancouver, B.C.) with collection of unlabeled T cells (typically >96% $CD4^+$ and > 90% viable as assessed by flow cytometry). Purified $CD4^+$ cells were cultured in RPMI/10% FBS at 2×10^5 cells/well in 200 μL total volume in 96-well microtiter plates. The Jurkat and Hut-78 T cell lines (ATTC, Rockville, MD) were cultured in RPMI 1640 supplemented with 10% FBS (Jurkat) or 20% FBS (Hut-78) and 2 mM L-glutamine, 1.5g/L sodium bicarbonate, 4.5 g/L glucose, 10 mM HEPES, and 1.0 mM sodium pyruvate. Cells were maintained in log phase at 37 ^{0}C and 5% CO_2 and

seeded at 1 x 10^5 cells/well in 96-well plates for individual experiments. To prevent overgrowth in co-culture experiments, Jurkat cells were seeded at 5 x 10^4 cells/well and primary T cells were seeded at 1 x 10^5 cells into the same well.

Cell Viability and Flow Cytometry Staining

Methods of immunofluorescent staining and flow cytometry were performed as previously described (Coligan, 1995). Briefly, cells were stained with fluorescently labeled antibodies (Beckman Coulter, Miami, FL) for 30 minutes at 4^{o}C, washed two times, and immediately analyzed on a 3-color Epics flow cytometer (Beckman Coulter). Five to ten thousand events gated on size (forward scatter-FS) and granularity (side scatter-SSC) were analyzed, and expression of the percentage of positively staining cells or the mean fluorescence intensity (MFI) was determined by comparisons to isotype controls. Appropriate concentrations of each antibody were determined by titration for optimal staining prior to experimental use.

To assess cell viability, two different assays were employed. In the first assay, T cells were dually stained with fluoroscein isothiocyanate labeled antibodies (anti-CD4 for primary T cells and anti-HLA ABC for T cancer cell lines) followed by treatment with 50 μg/mL propidium iodide (PI) to monitor losses in membrane integrity. After 10 min of PI staining, fluorescent CountBright counting beads (Invitrogen, Carlsbad, CA) were added to samples to enable determinations of absolute cell numbers, and changes in PI staining used to quantify cell death. Nanoparticles were excluded from analysis based on the absence of fluorescence signal and light forward scatter (FS) and side scatter (SSC) characteristics. A second viability assay, the LIVE/DEAD viability assay for mammalian

cells (Invitrogen, Eugene, OR), was used to verify results. Per manufacturer's protocol for flow cytometry, cells were dually stained with two fluorescently labeled probes that enable the simultaneous determination of live and dead cells in a sample. Calcein AM was used to stain live cells as it fluoresces only when cleaved by intracellular esterases and EthD-1 was used to identify dead/dying cells as it exclusively enters cells with disrupted cell membranes.

In co-culture experiments, Jurkat cells and primary T cells were distinguished from each other using differential gating based on their differing and non-overlapping light scattering properties indicative of size (FS) and granularity (SSC) between the two cell types. FS and SSC of Jurkat cells was ~ 2.2 and 3.2 times greater than for primary T cells, respectively.

ROS Production

To assay for reactive oxygen species (ROS) production, primary human T cells were treated with the oxidation-sensitive dye, 2', 7'-dichlorofluorescein diacetate (DCFH-DA; Invitrogen, Carlsbad, CA). The oxidation product of DCFH-DA has an excitation/emission maxima of ~495 nm/529 nm enabling detection using standard flow cytometry. Whole blood was treated with an ammonium chloride solution (1.5 M NH_4Cl, 0.1 M $NaHCO_3$, 0.01 M EDTA) to lyse red blood cells and centrifuged for 10 min at 4^oC to remove erythrocytic debris. The white blood cells were then resuspended in phenol red-free RPMI a 2 x 10^5 cells/well and treated with 13 nm ZnO NP. After 18 h of treatment, cultures were loaded with 5 μM of DCFH-DA for 20 min and ROS production evaluated using flow cytometry as previously described (Luo et al., 2002). To ensure

cells were capable of ROS production, control samples were activated with 25 ng/mL of PMA for 1 h after loading with DCFH-DA. White blood cell populations (i.e., T lymphocytes and monocytes) were distinguished by FS and SSC characteristics and staining with fluorescently-labeled antibodies (e.g., CD3, CD14). ROS production was also performed in Hut-78 cells using similar methodology.

ROS Quenching

To determine the role of ROS in NP-induced cell death, Jurkat leukemia cells were seeded in a 96-well plate at 0.2 mL per well at a concentration of 1×10^5 cells/well. A stock solution of N-Acetyl Cysteine (NAC, Sigma Aldrich) was made in sterile nanopure water and added to cells at 5 mM or 10 mM for 1 h. After NAC pretreatment, cells were cultured with 0.3-0.5 mM ZnO NP for 24 h. Viability was determined by PI exclusion and flow cytometry with fluorescent CountBright counting beads (Invitrogen, Carlsbad, CA) added to samples to enable determination of absolute cell numbers.

Statistical Analyses

All data was analyzed using SAS, Inc. software (Cary, N.C.). Data for Figure 1A and 2 were analyzed using repeated measures of variance with post hoc comparisons and significance levels defined as $p<0.05$. Repeated measures of variance analyses were used when two or more measurements of the same type were made on the same subject to determine statistical differences between the means and allow within-subject variation to be separated from between-subject variation. Data for Figures 1B and 5 were analyzed using a two-way analysis of variance (ANOVA) to test for statistical significance of the

model and post hoc comparisons were used to test for statistically significant effects of treatment on cell viability ($p<0.05$).

Results

Preferential Killing of Cancerous Cells by ZnO NP

Experiments in our lab have previously shown that T cells activated through the T cell receptor and its CD28 costimulatory pathway were more susceptible to ZnO NP toxicity (Hanley et al., 2008). We hypothesized that this susceptibility was due to the proliferation increase that occurs upon activation. In light of this, experiments were performed to determine whether continuously dividing cancer cells display an even greater sensitivity to ZnO NP toxicity. Jurkat leukemic and Hut-78 lymphoma T cell lines were treated with ZnO NP for 24 h and viability was determined by PI uptake. Both T cell cancer lines displayed strikingly greater (28-35 fold) sensitivity to NP toxicity compared to resting normal T cells (Figure 2.1). Significant differences were observed between Hut-78 and normal T cells ($p=.0101$ and 0.0434 at 1 mM and 5 mM NP, respectively) and Jurkat and normal T cells (<0.0001 at both 1 mM and 5 mM NP). An IC_{50} of ~0.17 mM was observed for Hut-78 cells and ~0.21 mM for Jurkat T cells. No appreciable loss of primary T cell viability was observed at NP concentrations (e.g., 0.5 mM) that effectively killed the cancerous T cells.

To validate experimental results, a second viability assay was employed. Similar experiments were performed using the LIVE/DEAD viability assay (Invitrogen, Eugene, OR), which allows for the simultaneous determination of live and dead cells in a sample

by labeling live cells with the Calcein AM dye that fluoresces only when cleaved by intracellular esterase enzymes and the vital dye, EthD-1, which only enters dead/dying cells with disrupted cell membranes. As shown in Figure 2.1B, nearly identical results were obtained using this independent assay for viability, with ZnO NP displaying preferential toxicity against cancerous cells compared to normal cells of identical lineage. It should be noted that no statistically significant change in primary T cell viability occurs between untreated control cells and cells treated with low NP concentrations (0.2 and 0.5 mM), while a significant decrease ($p<0.0001$) in Jurkat leukemia cell viability can readily be seen at the lowest concentration tested (~52% viable/48% dead at 0.2 mM) with no live cancer cells detectable at 5 mM NP.

To verify that preferential cancer cell killing occurs in the direct presence of normal healthy T cells, co-culture experiments were performed. For these experiments, Jurkat T cells were co-cultured with primary $CD4^+$ T cells, treated with various concentrations of ZnO NP for 24 h, and cell viability assessed by PI uptake. Figure 2.2 confirms the preferential killing of cancerous Jurkat T cells with a very similar IC_{50} value being observed for co-cultured Jurkat cells (IC_{50} ~0.28 mM) compared to these cells cultured alone (Figure 2.1). Again, only very limited cytotoxicity was observed on co-cultured normal T cells at corresponding NP concentrations with significant differences ($p<0.0001$) between cell types being observed at 0.3, 0.4, and 0.5 mM NP concentrations.

Kinetics of ZnO NP-Mediated Toxicity

Additional experiments were performed to determine the kinetics of ZnO NP toxicity in both primary and cancerous T cells. Because primary and immortalized T cells have markedly different sensitivities to ZnO NP, concentrations were chosen for each cell type (10 mM for primary T cells and 0.5 mM for Jurkat T cells) that produce at least 75% cytotoxicity by 24 h exposure. As shown in Figure 2.3, both primary T cells and Jurkat cells displayed similar kinetics, with appreciable loss of cell viability beginning as early as 8 h post treatment and full toxicity effects requiring a longer treatment period of 24 h.

ZnO NP Induce ROS Production

Several types of nanomaterials including quantum dots and metal oxide NP have been shown to induce the generation of excess reactive oxygen species (ROS) resulting in modification and damage of cellular proteins, DNA, and lipids, which can lead to cell death (Lovric et al., 2005; Xia et al., 2006; Green and Howman, 2005). To investigate oxidative stress produced by ZnO NP as a mechanism of cellular toxicity, experiments were performed using the cell permeable dye, DCFH-DA. In the presence of reactive oxygen species, including hydrogen peroxide and superoxide anion, DCFH-DA is oxidatively modified into a highly fluorescent derivative that is readily detectable using flow cytometry. As shown in Figure 2.4, a modest increase in DCF fluorescence was observed after 18 h of 5 mM ZnO NP exposure in primary lymphocytes (~7.0 fold increase – 12.5/1.78) and an even stronger induction observed in Hut-78 T leukemic cells at 24 h (~ 14.0 fold increase). Increased ROS production was detectable as early at 8 h of

NP exposure although greater levels were apparent at 18-24 h (data not shown). Because of the differing size and granularity properties of the cell types examined, different instrument voltage parameters were required, which prevents direct comparisons of intrinsic levels of ROS between cell types.

Role of ROS in NP-Induced Cytotoxicity

Experiments were performed to determine if the T cell death that results from NP exposure is dependent on the generation of intracellular ROS. Jurkat cells were exposed to increasing concentrations of the antioxidant and ROS quencher, NAC (N-acetyl cysteine), prior to treatment with NP for 24 h (Boudreau et al., 2007; Han et al., 2004). Figure 2.5 shows that NAC has significant effects to prevent NP-induced cytotoxicity with rescue being observed at both NP concentrations tested. Significant differences ($p<0.0001$) were observed between cultures not pretreated with NAC and both NAC pretreatments (5 mM and 10 mM) for each NP concentration tested. For example, with 10 mM NAC, nearly 100% viability was retained even at an NP concentration previously shown to reduce cell viability below 10%. These results indicate that ROS generation plays a causal role in NP-induced cytotoxicity.

Discussion

In this study we examined the toxicity profiles of human primary cells and transformed tumor cells to ZnO NP. Because cellular response is dynamic and the ultimate phenotype is affected by a myriad of competing or overlapping signals present in the microenvironment, studies were performed to determine how ZnO NP affect

quiescent cells compared to rapidly dividing tumor cells and whether different activation stimuli result in different toxicity responses. Here we present novel findings demonstrating that cancerous T cells are markedly more susceptible (~28-35 times) to ZnO NP mediated toxicity than their normal counterparts (Figure 2.1). These findings may be of important clinical interest as one of the greatest challenges facing chemotherapy is the inability of anticancer drugs to effectively distinguish between normal and transformed tissue (Nie et al., 2007; Hellman, 1980). Although many commonly used chemotherapeutic drugs target rapidly dividing cells, many suffer from a relatively low therapeutic index, that is, the ratio of toxic dose to effective dose (Bosanquet and Bell, 2004; Huang and Oliff, 2001). This limitation frequently causes a broad range of toxicities, leading to dose limiting toxicity and a concomitant reduction in antitumor efficacy. Importantly, the preferential toxicity of ZnO NP towards cancerous T cells is of substantial magnitude, especially in comparison to *ex vivo* indices reported for other commonly used chemotherapeutic agents using similar cell viability assays. Therapeutic indices of ≤ 10 have been reported for both doxorubicin and carboplatin against a variety of tumors, including acute myelogenous leukemia, non-Hodgkin's lymphoma, ovarian, and other solid tumors (Bosanquet and Bell, 2004). Thus, the inherent differential toxicity of ZnO NP against rapidly dividing cancer cells raises exciting opportunities for their potential use as anticancer agents, and the selectivity of these nanomaterials can be expected to be even further enhanced by design by linking tumor targeting ligands such as monoclonal antibodies, peptides, and small molecules to tumor-associated proteins, or by using NP for drug delivery.

The preferential killing of rapidly dividing cancer cells relative to quiescent cells of the same lineage suggests that mechanisms of ZnO NP toxicity might be related to the proliferative potential of the cell. Thus, we hypothesize that other highly proliferative cancerous cell types may show similar susceptibility to this cytotoxicity compared with their normal counterparts.

A number of studies indicate that certain nanomaterials, including metal oxide NP, have the potential to exhibit spontaneous ROS production based on material composition and surface characteristics while other nanomaterials trigger ROS production only in the presence of select cell systems (Lovric et al., 2005; Xia et al., 2006; Long et al., 2006). Results from our flow cytometry experiments provide evidence of ROS production in a biotic environment following ZnO NP exposure. These findings have important implications regarding mechanisms of cellular toxicity as elevated ROS production that exceeds the capacity of the cellular antioxidant defense system causes cells to enter a state of oxidative stress, which results in damage of cellular components such as lipids, proteins, and DNA (Lovric et al., 2005; Xia et al., 2006). The oxidation of fatty acids then leads to the generation of lipid peroxides that initiate a chain reaction leading to disruption of plasma and organelle membranes and subsequent cell death. We observed a concentration and time-dependent increase in ROS production in primary T cells following ZnO NP exposure (Figure 2.4), with even higher levels being observed in immortalized T cells. This may mechanistically underlie the greater susceptibility of cancerous T cells to NP-mediated toxicity. Indeed, studies using the ROS quencher,

NAC, demonstrated the causal role of ROS generation in NP-mediated cytotoxicity (Figure 5).

Conclusion

The key findings of this work support the view that ZnO NP induce toxicity in a cell-specific and proliferation dependent manner with rapidly dividing cells being the most susceptible and quiescent cells being the least sensitive. The marked difference in cytotoxic response between cancer cells and their normal counterparts suggests an exciting potential for ZnO NP as novel alternatives to cancer chemotherapy and radiation therapy.

References

Bosanquet, A.G., and Bell, P.B. (2004). Ex vivo therapeutic index by drug sensitivity assay using fresh human normal and tumor cells. J. Exp. Ther. Oncol. 4, 145-154.

Boudreau, R.T., Conrad, D.M., and Hoskin, D.W. (2007). Differential involvement of reactive oxygen species in apoptosis caused by the inhibition of protein phosphatase 2A in Jurkat and CCRF-CEM human T-leukemia cells. Exp. Mol. Pathol. 83, 347-356.

Coligan, J.E. (1995). Current Protocals in Immunology. (New York: Greene Publishing Associates and Wiley-Interscience).

Green, M., and Howman, E. (2005). Semiconductor quantum dots and free radical induced DNA nicking. Chem. Commun. (Camb) 1, 121-123.

Groneberg, D.A., Giersig, M., Welte, T., and Pison, U. (2006). Nanoparticle-based diagnosis and therapy. Curr. Drug Targets 7, 643-648.

Han, S., Espinoza, L.A., Liao, H., Boulares, A.H., and Smulson, M.E. (2004). Protection by antioxidants against toxicity and apoptosis induced by the sulphur mustard analog 2-chloroethylethyl sulphide (CEES) in Jurkat T cells and normal human lymphocytes. Br. J. Pharmacol. 141, 795-802.

Hanley, C., Layne, J., Punnoose, A., Reddy, K.M., Coombs, I., Coombs, A., Feris, K., and Wingett, D. (2008). Preferential killing of cancer cells and activated human T cells using ZnO nanoparticles. Nanotechnology 19, 295103.

Hellman, S. (1980). Improving the therapeutic index in breast cancer treatment: the Richard and Hinda Rosenthal Foundation Award lecture. Cancer Res. 40, 4335-4342.

Huang, P.S., and Oliff, A. (2001). Drug-targeting strategies in cancer therapy. Curr. Opin. Genet. Dev. 11, 104-110.

Lanone, S., and Boczkowski, J. (2006) Biomedical applications and potential health risks of nanomaterials: molecular mechanisms. Curr. Mol. Med. 6, 651-663.

Long, T.C., Saleh, N., Tilton, R.D., Lowry, G.V., and Veronesi, B. (2006) Titanium dioxide (P25) produces reactive oxygen species in immortalized brain microglia (BV2): implications for nanoparticle neurotoxicity. Environ. Sci. Technol. 40, 4346-4352.

Lovric, J., Cho, S.J., Winnik, F.M., and Maysinger, D. (2005) Unmodified cadmium telluride quantum dots induce reactive oxygen species formation leading to multiple organelle damage and cell death. Chem. Biol. 12, 1227-1234.

Luo, J., Li, N., Paul, R.J., and Shi, R. (2002). Detection of reactive oxygen species by flow cytometry after spinal cord injury. J. Neurosci. Methods 120, 105-112.

McNeil, S.E. (2005). Nanotechnology for the biologist J. Leukoc. Biol. 78, 585-594.

Nel, A., Xia, T., Madler, L., and Li, N. (2006) Toxic potential of materials at the nanolevel. Science 311, 622-627.

Nie, S., Xing, Y., Kim, G.J., and Simons, J.W. (2007). Nanotechnology applications in cancer. Annu. Rev. Biomed. Eng. 9, 257-288.

Reddy, K.M., Feris, K., Bell, J., Wingett, D.G., Hanley, C., and Punnoose, A. (2007) Selective toxicity of zinc oxide nanoparticles to prokaryotic and eukaryotic systems. Applied Physics Letters 90, 213902-213903.

Xia, T., Kovochich, M., Brant, J., Hotze, M., Sempf, J., Oberley, T., Sioutas, C. Yeh, J.I., Wiesner, M.R., and Nel, A.E. (2006). Comparison of the abilities of ambient and manufactured nanoparticles to induce cellular toxicity according to an oxidative stress paradigm. Nano. Lett. 6, 1794-1807.

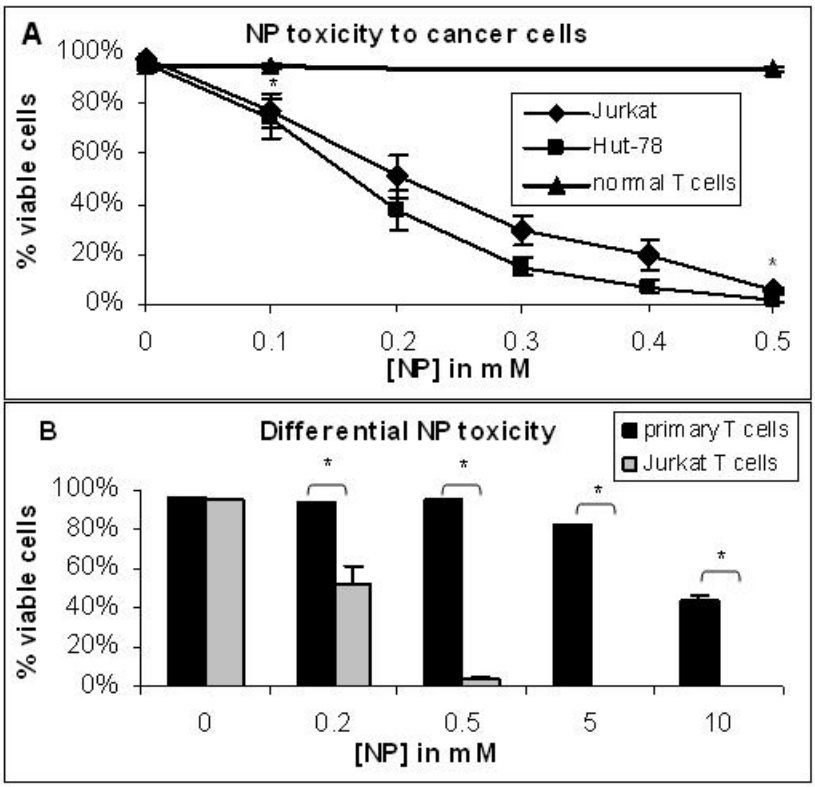

Figure 2.1. Differential cytotoxic effects of ZnO NP on cancerous T cell lines and primary T cells (Hanley et al., 2008). **A)** Jurkat, Hut-78 T cell lines, or normal primary T cells were treated with varying concentrations of ZnO nanoparticles for 22-24 h and viability determined by monitoring PI uptake using flow cytometry as described for Figure 1. Data from seven (Jurkat), three (Hut-78), and four (normal $CD4^+$ T cells) independent experiments is presented and error bars depict standard error. Data was analyzed using a repeated measures ANOVA and model based means post test. Statistical comparisons were made between each cancer cell line and primary T cells at 0.1 mM and 0.5 mM ZnO NP with significance levels defined as $p<0.05$ and indicated by an asterisk. **B)** Jurkat and primary T cell viability was assessed using the LIVE/DEAD® Viability/Cytotoxicity Kit for mammalian cells (Invitrogen, Eugene, OR). Following ZnO NP exposure for 24 h, cells were stained with calcein AM (green fluorescence) and ethidium homodimer-1 (red fluorescence) to differentiate between live and dead cells, respectively. Data from a representative experiment is presented with error bars depicting standard error, n=3. A two-way analysis of variance combined with a model based means test indicates significant differences in viability between Jurkat and primary T cells for all NP concentrations tested (asterisk denotes $p<0.0001$).

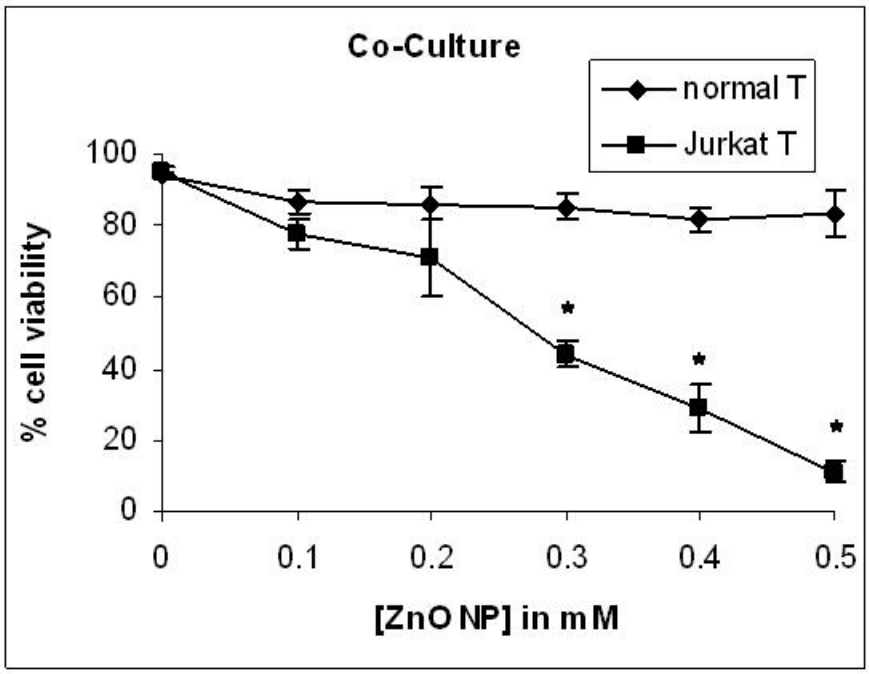

Figure 2.2. Viability effects of ZnO NP on co-cultures of cancerous and normal T cells. Individual wells in a 96-well plate were seeded with Jurkat and primary T cells and treated with various concentrations of ZnO nanoparticles for 22-24 h. Viability was determined by monitoring PI uptake using flow cytometry. Data from three independent experiments is presented and error bars depict standard error. Statistical analysis was performed using a repeated measures ANOVA and model based means post hoc test. Significance levels were defined as $p<0.05$ and are indicated by an asterisk.

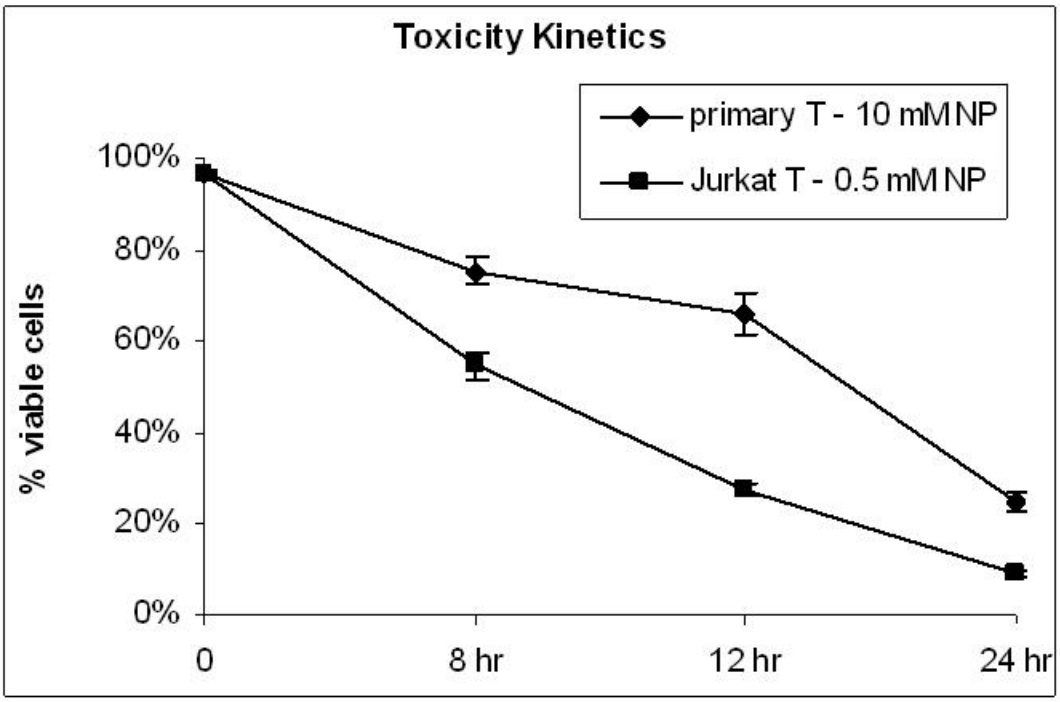

Figure 2.3. Kinetics of ZnO NP toxicity on immortalized and primary human T cells (Hanley et al., 2008). Freshly isolated $CD4^+$ T cells (purity > 96%) were treated with 10 mM ZnO NP and Jurkat T cells were treated with 0.5 mM ZnO NP for varying times and viability determined using PI uptake and flow cytometry. Means ± standard error from representative experiments are presented (n=3).

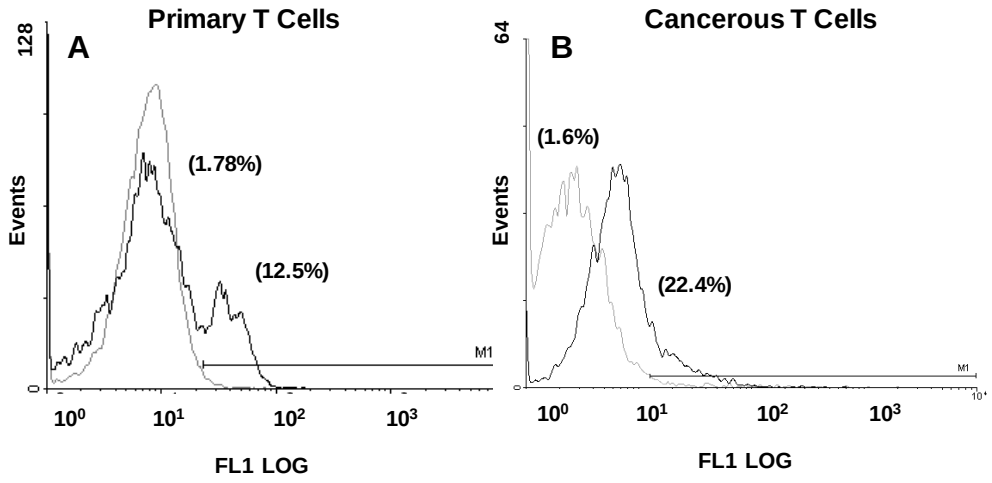

Figure 2.4. Cellular production of ROS following ZnO NP exposure (Hanley et al., 2008). ROS generation was evaluated in primary T cells and in the transformed Hut-78 T cell line following 18-24 h of ZnO NP exposure using the oxidation sensitive dye DCFH-DA and flow cytometry. **A)** Representative histograms depicting ROS production in primary T cell. Assays were performed using freshly obtained whole blood in which red blood cells were removed following NH_4Cl lysis. T lymphocytes were gated based on staining with fluorescently labeled CD3 antibodies and the oxidation product of DCFH-DA detected using the FL1 detector. **B)** Histogram depicting ROS production in the transformed Hut-78 T cell line. In each histogram, the light grey line depicts background fluorescence in DCFH-DA loaded cells while the black line depicts fluorescence in DCFH-DA loaded cells treated with ZnO NP for 18 h (A) or 24 h (B). To assess relative increases in ROS following NP treatment, a marker (M1) was set so that background fluorescent in control samples (DCFH-DA loaded/no NP) was between 1.5 and 2% and numbers in parentheses indicate the percentage of fluorescence positive cells.

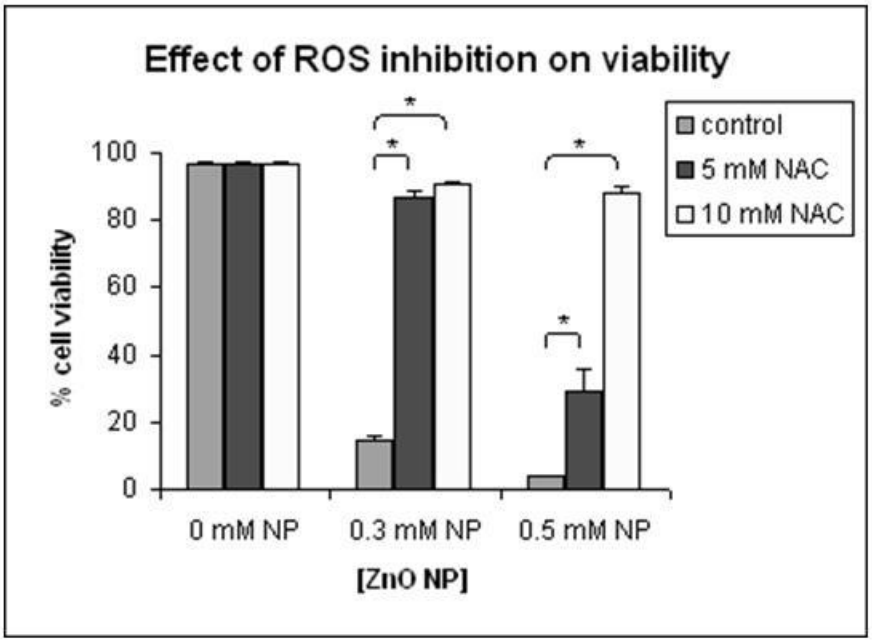

Figure 2.5. Quenching of ROS protects against NP-mediated cytotoxicity. Jurkat cells were pretreated with 5-10 mM N-acetyl cysteine for 60 min and then treated with 0.3-0.5 mM ZnO NP. After 24 h, cell viability was determined using propidium iodide exclusion and flow cytometry. Data from a representative experiment performed in triplicate is presented with error bars depicting standard error. A two way analysis of variance was performed followed by a model based means test to show significant differences in means of cell viability (%) between treatments (asterisk denotes $p<0.0001$).

CHAPTER 3: SELECTIVE CYTOTOXICITY OF ZINC OXIDE NANOPARTICLES TO CANCEROUS CELLS: THE ROLE OF PROLIFERATION, NANOPARTICLE ELECTROSTATICS, AND DISSOLUTION PROPERTIES

Introduction

Nanoparticles (NP), substances with dimensions of 1 to 100 nm, are being increasingly investigated for their utility in diverse fields ranging from microelectronics, accelerating degradation of water pollutants via photocatalytic activity, food additives, cosmetics, sunscreens, as well as a variety of biological applications (Nel et al., 2006). These novel applications are enabled by the new physical, chemical, and magnetic properties that can emerge when materials are reduced to the nanoscale (Lanone and Boczkowski, 2006). Particular interest has arisen in the utility of NP in the area of medicine, now termed "nanomedicine," because the similar size of NP to naturally occurring biological molecules can facilitate their entry into cells and subsequent interactions with proteins, nucleic acids, or other biomolecules (McNeil, 2005). Based on the new properties that can sometimes accompany the reduction of materials down to the nanoscale, nanomedicine seeks to deliver a new set of tools, devices, and therapies for the treatment of human diseases. With respect to cancer, the small size of NP can take advantage of the enhanced permeability and retention (EPR) effect, which is recognized as a "gold standard" in the design of new chemotherapy agents, allowing for the intra-tumor accumulation of therapeutic agents due to a combination of increased vascular

permeability and poor lymphatic drainage (Cho et al., 2008). This localized imbalance in the tumor microenvironment allows NP of certain sizes to readily enter, but to be passively retained within the tumor interstitial space (Cho et al., 2008). In addition, as NP become smaller, their surface area to volume ratio increases, which results in a greater percentage of atoms on the particle surface and can make previously benign substances highly reactive (Nel et al., 2006). The increased number of reactive atoms at the particle surface also creates more sites to conjugate drugs or targeting molecules to the particle (Nie et al., 2007), providing an effective drug-delivery platform for existing chemotherapeutics, as well as new approaches for using NP in whole tumor imaging applications (Ferrari, 2005).

The use of nanomaterials in anti-cancer applications is receiving considerable interest in the scientific community, as there is a pressing need to develop new and improved chemotherapeutics that effectively kill cancerous cells while reducing unwanted side effects to normal body tissues. Currently used cancer therapies often fail to effectively discriminate between cancerous and normal cells, which can lead to a number of systemic toxic side effects, including myelosuppression, neurotoxicity, and cardiomyopathy (Nie et al., 2007; Bosanquet and Bell, 2004). Recently, studies from our lab have demonstrated the ability of ZnO NP to preferentially kill cancerous T cells, showing more than a 30-fold greater *in vitro* cytotoxicity to cancer cells than to corresponding normal cells (Figure 2.1; Hanley et al., 2008). Importantly, the selective cancer cell toxicity represents an intrinsic property of ZnO NP, which may enable further improvements in their therapeutic potential via conjugation with existing chemotherapy

agents or cancer-targeting ligands.

Prior to the development of ZnO NP for cancer applications, it is necessary to demonstrate that their inherent cancer selective properties extend beyond T cell malignancies. A better mechanistic understanding is also needed, both regarding the characteristics of cancerous cells and the properties of NP that are responsible for this selectivity. The study described in this chapter aims to determine the extent to which cancerous cells from multiple lineages are preferentially killed by ZnO NP, and to elucidate the role of cell proliferation, NP dissolution and electrostatic properties, and ROS generation in the toxicity mechanism. This knowledge is expected to help guide future NP modifications to improve their therapeutic potential.

Materials and Methods

Preparation and Characterization of Zinc Oxide Nanoparticles

Two different types of ZnO NP were synthesized and used in this work. The first type, used throughout the study and referred to in the particle charge experiments as ZnO I, was prepared using a procedure in which the zinc acetate dihydrate precursor was hydrolyzed in DEG solution with water. For this, 1.00g (4.56 mmol) of zinc acetate dihydrate was dissolved in 100 mL of diethylene glycol (DEG) while under constant stirring and heated to 80º C. Then, a select amount of nanopure water was added drop wise to the solution, which was then heated to 160º C and maintained for 1.5 hours. After cooling, the NP in the resulting milky white solution were centrifuged and washed with ethanol 3-5 times to remove the solvent. The NP were dried for 12 h at 50º C.

A separate set of ZnO NP (referred to as ZnO II and used only for particle charge experiments) were prepared using a different synthesis procedure by hydrolyzing zinc acetate hydrate in anhydrous ethanol with LiOH solution. 1.10 g of zinc acetate hydrate (5.01 mmol) was added to a round bottom flask containing 100 mL of anhydrous ethanol and heated under constant stirring. After attaining a reaction temperature of 70º C, 100 mL of 0.1M LiOH (in ethanol) was added to the flask, stirred for another 10 min, and allowed to age for 12 h. The resulting colloid was centrifuged and washed with ethanol and n-heptane before drying for 12 h at 50 °C. The ZnO NP chemical phase, crystallite size (8-13 nm) and shape were confirmed using x-ray diffraction (XRD), transmission electron microscopy (TEM), and spectrophotometry (Reddy et al., 2007). Zeta potentials of the powdered samples of ZnO I and ZnO II were measured in nanopure water with a Malvern Zetasizer NanoZS at 25^0C. The NP were then reconstituted in phosphate buffered saline (PBS). After reconstitution, NP were sonicated for 10 min and immediately vortexed before addition to cell cultures.

Peripheral Blood Mononuclear Cell and Red Blood Cell Isolations

Whole blood was obtained from donors with informed consent and University Institutional Review Board approval. Peripheral blood mononuclear cells (PBMC) were obtained by Ficoll-Hypaque (Histopaque-1077, Sigma, St. Louis, MO) gradient centrifugation using heparinized phlebotomy samples (Coligan, 1995). Cells were washed 3 times with Hank's buffer (Sigma) and incubated at 1 x 10^6 cells/mL in RPMI-1640 (Sigma) containing 10% fetal bovine serum (FBS). Red blood cells were isolated from whole blood via centrifugation at 2000 rpm at 4^0C for 10 min. The cells were

washed with phenol red-free RPMI media four times and resuspended at $5x10^8$ cells/ml. Primary lymphocytes were tested for NP cytotoxicity in PBMC cultures, but identified from other cell types present in the mixture based on gating for cells staining $CD19^+$/ $CD3^-$ for B cells, and $CD4^+$ /$CD3^+$ for T cells.

Cell Culture

PBMCs, red blood cells (RBC), Jurkat, Daudi, K562, and T47D (ATCC, Manassas, VA) were cultured in RPMI media supplemented with 10% FBS, 2 mM L-glutamine, 2.0 g/L sodium bicarbonate and 3.575g/L HEPES for PBMCs, and 1.5g/L sodium bicarbonate, 4.5 g/L glucose, 2.6 g/L HEPES, and 1.0 mM sodium pyruvate for Jurkat, Daudi, T47D and RBCs. PC3 prostate cancer cells (ATCC, Manassas, VA) were cultured in F-12K Kaighn's modification of Ham's medium supplemented to contain a final concentration of 10% fetal bovine serum. Primary Human Mammary Epithelial Cells (HMEC; Lonza, Allendale NJ) and MCF10A (ATCC) were grown in complete MEGM media (Lonza). 100 ng/mL cholera toxin was added to MCF10A media to stimulate cell proliferation. Prostate Epithelial Cells (PrEC) were cultured in complete PrEGM (Lonza). All cells were incubated at 37 C with 5% CO_2. Adherent cells were maintained at 30 – 80% confluence and suspension cells were maintained in log growth phase.

Viability Assays

To determine the cytotoxicity of ZnO NP, cells were incubated with various concentrations of NP suspended in phosphate buffered saline (PBS) and sonicated for 15-

20 min. After 24 h NP treatment, cell viability was assessed using either propidium iodide (PI) dye exclusion assay to monitor losses in membrane integrity (Invitrogen) or an Alamar Blue reduction assay. All cell lines were cultured in their recommended media, but NP treated in the RPMI-based media to reduce effects of media components on NP surface characteristics (i.e. protein coating, pH, etc.). For the PI exclusion assay, cancerous B and T cell lines were stained with fluoroscein isothiocyanate labeled antibodies to HLA ABC, while primary B and T cells present in mixed PBMC cultures were identified by staining with anti-CD4, anti-CD19, and anti-CD3 antibodies (Beckman Coulter, Miami, FL) for 30 min at 4°C. After washing, cells were stained with 50 μg/mL PI for 10 min, followed by the addition of fluorescent CountBright counting beads (Invitrogen, Carlsbad, CA) to enable determination of absolute cell numbers. Flow cytometry was used to evaluate changes in PI staining in relevant cell populations ($CD19^+$, $CD3^-$ B cells and $CD3^+$, $CD4^+$ T cells) by analyzing ten thousand events on a 4-color Epics flow cytometer (Beckman Coulter). Nanoparticles were excluded from analysis based on the absence of a fluorescence signal and light forward scatter (FS) and side scatter (SSC) characteristics.

An Alamar Blue assay was used to confirm results from PI staining and determine viability in adherent cell lines. Reduction by mitochondrial enzymes in metabolically active (live) cells causes Alamar Blue to fluoresce, with excitation/emission wavelengths at 530/590 nm. Adherent cells were seeded into 24 well plates at 4×10^4 cells/well to prevent confluence and NP treated. Alamar Blue was added to samples at 10% by volume and incubated for ~ 4 h, and fluorescence changes read on a spectrophotometer after 24 h

NP exposure. Viability was calculated as percent of fluorescence of untreated control samples.

K562 cells were plated in 24 well plates at 1.2 x 10^5 cells/well, treated with NP, and viability determined using the Alamar Blue assay. Red blood cell toxicity was assessed via hemolytic activity determined by hemoglobin release. Cells were mixed 1:1 with different concentrations of NP (75 ul:75 ul), samples incubated for 24 h, and cells centrifuged at 2000 rpm for 10 min to remove debris. The absorbance of hemoglobin released in the supernatant was measured at 540 nm. Sample hemolysis was normalized to a positive control (1% Triton-X), and absorbance of NP in solution was subtracted from all samples. The effect of NP on RBC lysis was verified using an LDH assay which measures the conversion of pyruvate to lactate in the presence of NADH (Stagsted and Young, 2002). After NP treatment, the plate was centrifuged at 2000 rpm for 10 min, 75 ul of the supernatant transferred to a new plate, and 0.1 M Tris/HCL, 0.1% NADH and 0.15M pyruvate added to the sample. Cytotoxicity was expressed as change in absorbance of LDH at 340 nm.

Proliferation Rate Assay

The Alamar Blue assay was used to determine the proliferation rates of Jurkat, T47D, HMEC, and primary T cells given the recognized correlation between Alamar Blue reduction and cell number (Al Nasiry et al., 2007; Zhi-Jun et al., 1997). T47D, Jurkat, and primary T cells were plated at a concentration of 2 x 10^4 cells/well in 24-well plates. HMEC were plated at 4 x 10^3 cells/well to prevent confluence due to their large

size. Alamar Blue (10% by volume) was added to wells assigned for each day for 4 days and incubated for 4 h. The fluorescence at 590 nm was read on a spectrophotometer and plotted against time. For each time interval in the experiment (~24 h), a ratio of fluorescence was calculated (end fluorescence value/beginning fluorescence value), and used to calculate a doubling time (Fl. Ratio/24 h = 2/x hours). Three data points each averaged from a triplet experiment are compared for Jurkat and primary T cells, while eight (T47D) data points are compared with nine (HMEC), and six (PC3) data points are compared with eight (PrEC) for epithelial cell lines.

Proliferation Inhibitors

Inhibition of cell proliferation was performed using chemical inhibitors or growth factor starvation. To arrest Jurkat cells in G_0, cells were plated at 1 x 10^5 cells/well in media containing 2% FBS. After 24 h, cells were centrifuged, resuspended in media containing 10% FBS at 1 x 10^5 cells/mL, and treated with 0.25 mM NP for 24 h. Inhibition of proliferation in MCF10A cells was achieved by omitting epithelial growth factor and cholera toxin from the media. After overnight culture, cells were treated with NP for 24 h and the Alamar Blue assay used to verify the inhibition of proliferation had occurred and, in conjunction, used to assess NP cytotoxicity. Cell cycle inhibition in T47D and PC3 cells was performed using 20 ng/mL Nocodazole to arrest cells in the G_2 to M phase by inhibiting microtubule polymerization, or Colcemid (10ng/mL for T47D; 8 ng/mL for PC3) to synchronize cells in M phase via microtubule depolymerization. Cells were plated 24 h prior to NP treatment to allow adherence to the bottom of culture wells, followed by the addition of fresh media containing cell cycle progression inhibitors.

After 17-20 h, fresh inhibitor-free media was added, cells allowed to recover for 1-2 h, cultures treated with ZnO NP for 24h, and viability assessed via the Alamar Blue assay.

ROS Assays

Assessment of superoxide anion levels upon NP treatment was accomplished using the Mitosox Red indicator dye (Invitrogen, Carlsbad, CA). Both primary and Jurkat T cells were plated at 1 x 10^5 cells/well, treated with NPs for 16-18 h, and dually stained with anti-HLA ABC (Jurkat cells) or anti-CD4 (primary T cells) antibodies and 2.5 μM Mitosox Red for 30 min, then washed, resuspended, and analyzed using flow cytometry as described above. Positive control cells were pretreated 30 min with 5 μM Antimicin. For ROS scavenger assays, T47D and PC3 cells were plated at 4 x 10^4 cells/well, and treated with 2.5 to 10 mM N-acetyl cysteine (NAC) or 1 to 2 mM glutathione reduced ethyl ester (Glth) for 1-2 h to allow cellular uptake. Cells were subsequently treated with NP and viability assessed using the Alamar Blue assay.

Nanoparticle Dissolution Studies

Cell-impermeant Newport Green DCF Salt (Invitrogen) was used in the absence of cells to determine the extent that ZnO NP dissolve into free Zn^{2+} ions. Standard curves were generated by adding serial 1:10 dilutions in the range of 1 nM-10 mM of either $ZnCl_2$ or $ZnSO_4$ to black Corning 96 well-plates. Nanoparticles were then suspended at 10 mM in deionized water or phenol red-free cell media, allowed to dissolve for 24 h, and centrifuged for 20 min at 13,000 rpm to pellet NP. Supernatant from NP samples was added to the same plate and compared to serial dilutions of the two Zn^{+2} standard curves

in the range of 10 nM-10 mM. Newport Green was added to each well to a final concentration of 0.1 µM and fluorescence detected at 505/535 nm excitation/emission wavelengths. To determine the extent to which levels of zinc cations equivalent to those calculated to result from NP dissolution are responsible for toxicicity, cells were treated for 24 h with 0.05 mM $ZnCl_2$ and flow cytometry used to assess PI exclusion as described above.

To assess the effect of NP dissolution in the toxicity mechanism, NP were suspended in either PBS or RPMI media at 50 mM. NP were sonicated for 30 min and stored at room temperature for 24 h to allow dissolution. NP were then centrifuged for 20 min at 13,000 rpm, and cells treated with NP or supernatant equal to NP concentrations of 0.25 and 0.5 mM. After 24 h, cells were stained for flow cytometry as previously described and viability assessed via PI exclusion.

Endocytosis Assessment

Chemical inhibition of endocytosis was accomplished using Cytochalasin D, which is a general inhibitor of endocytosis via interference with actin filaments. Jurkat cells were incubated for 3 h with 1.5 µg/mL Cytochalasin D, resuspended in fresh media and treated with NPs for 24 h. Flow cytometry and PI exclusion was used to determine viability. For assays using adherent cultures, cells were plated and allowed to adhere to wells. After O/N culture, media containing endocytosis inhibitors was added for 3h, then replaced with fresh standard media, cells treated with NP for 16 h. Effects of NP treatment were determined using the Alamar Blue assay.

Statistical Analysis

All data was analyzed with SAS, Inc. software (Cary, N.C.) using analysis of variance (ANOVA) to test for statistical significance of the model and post hoc comparisons to test for statistically significant effects of treatments on cell viability ($p<0.05$).

Results

Previous research has shown that T cell leukemias and lymphomas are markedly more susceptible (~28-35 fold) to ZnO NP toxicity than normal T lymphocytes. These studies were extended to determine whether preferential cancer cell cytotoxicity was observed for other types of cancerous cells. As shown in Figure 3.1, cancerous B cells and breast cancer epithelial cells are more susceptible to ZnO NP-induced cytotoxicity compared to normal B cells and mammary cells. Normal and cancerous T cells were also included in these experiments as controls. Following treatment with 0.5 mM ZnO NP, both primary T and B cells remained ≥ 92% viable, while only 4.3% of cancerous T cells (Jurkat) and 22.9% of cancerous B cells (Daudi) remained viable (Figure 3.1A). Similarly, at 1 mM NP, primary T and B cells remained > 80% viable while cancerous cells showed near complete death (1.2-8.9% viable, respectively). In fact, at all common NP concentrations evaluated, primary lymphocytes were significantly more resistant compared to their cancerous counterparts ($p<.0001$). IC_{50} values for T and B cell malignancies were ~ 0.25 and 0.18 mM, respectively, while those for primary T and B cells were ~7.0 and ~4.0 mM, respectively. As shown in Figure 3.1B, primary mammary

epithelial cells (HMEC) were significantly more resistant (IC_{50} ~0.75 mM) to ZnO NP-induced cytotoxicity compared to T47D breast cancer cells (IC_{50} ~0.3 mM). T47D viability dropped to 56.5% with 0.25 mM NP treatment, while HMEC remained 83.9% viable. When treated with 0.5 mM NP, only 31% of T47D cells were alive compared to 65.1% in normal breast cells (p=.0198). Significantly less death (p=.0122) was also observed at 1 mM NP, with 1.9% T47D remaining viable compared to 38.7% in HMEC.

In contrast, Figure 3.1C shows no significant difference in susceptibility to ZnO NP toxicity between the prostate cancer cell line PC3 and their normal counterparts, prostate epithelial cells (PrEC) under the culture conditions evaluated. Both primary and malignant prostate epithelial cells show an IC_{50} of approximately 0.4 mM.

Experiments were then performed to evaluate ZnO NP effects on erythrocytes. Figure 3.2A shows that human red blood cells (RBC) are essentially resistant to ZnO NP at concentrations producing near complete death in immortalized and normal lymphocytes and epithelial cells. For example, at 10 mM ZnO NP concentrations, <1% of RBCs showed lysis using a hemoglobin release assay, with minimal loss in viability observed at the highest concentration (60 mM) evaluated. Experimental results were confirmed using an independent LDH (lactate dehydrogenase) release assay where a similar lack of significant toxicity was observed. In contrast, data in Figure 3.2B shows that K562 erythroleukemic cells are killed at considerably lower NP concentrations with an IC_{50} of ~0.57 mM. Collectively, these studies show that ZnO NP have different degrees of toxicity towards different types of cancers, with non-adherent hematopoietic malignancies showing the greatest susceptibility compared to corresponding normal cell

counterparts. It is important to note, however, that the observed differences in NP susceptibility between epithelial and hematopoietic cells may be related to differences in growth characteristics between adherent and suspension cells, and the effects of sedimented NP in contact with adherent cell membranes.

To gain insights into the mechanism of NP susceptibility, experiments were performed to determine the role that proliferative potential plays in the differential cytotoxicity mechanism. The Alamar Blue reduction assay was used in these studies to determine relative proliferation rates for various cancerous and normal cell types as previously described (Al Nasiry et al., 2007; Zhi-Jun et al., 1997). Figure 3.3A shows a significantly lower ($p<.0001$ for all time points) growth rate of primary T cells versus Jurkat leukemic T cells, in which no doubling occurred for primary T cells over a 96 h period, while Jurkat cell doubling time was ~ 23.6 +/- 4.1 h. Control experiments using vital dye staining verified that the lack of Alamar reduction in primary T cells reflected quiescence rather than cell death, with greater than 95% viability observed on Day 0 and 65-70% viability observed on Day 3. Similar studies were performed on normal and cancerous breast epithelial cells (Figure 3.3B). As expected, the immortalized cells showed a greater proliferation rate (29.3 +/- 1.1 h) than primary epithelial cells (35.1 +/- 1.7 h), although the difference was less striking than observed for T lymphocytes (Table 3.1). When proliferation rates were compared between cancerous and normal prostate cells, however, no differences were found (Figure 3.3C); PrEC showed a 35.3 +/- 1.3 h doubling time, while PC3 doubled in 35.3 +/- 1.7 hours (Table 3.1). Comparison of the IC_{50} values with proliferation rates for the various cell types indicates that susceptibility

to NP cytotoxicity is closely tied to proliferation rate (Table 3.1).

Experiments were then performed to determine the role that cell cycle progression plays in NP susceptibility using cell cycle inhibitors or growth factor deprivation. Serum deprivation was used to halt Jurkat cell proliferation in the G_0 phase of the cell cycle. Experiments demonstrated (Figure 3.4A) that cell viability remained relatively unaffected by serum deprivation in control cultures (~93% viable), while 0.25 mM ZnO NP treatment in serum-deprived cells led to a significantly greater resistance to NP-induced cytotoxicity compared to exponentially growing cells (88.9 +/– 8.7% vs. 62.8% +/– 9.7%, p=0.0266). Control experiments verified that serum starvation resulted in the expected reduction in cell growth (Figure 3.4B), and vital dye staining was used to verify that cells remained viable up to 3 days (>95% viable, data not shown). Using a similar approach, the growth rate of breast epithelial MCF10A cells was modulated by culturing cells in media in the absence or presence of epithelial growth factor (EGF) and cholera toxin, both of which increase the proliferation rate of these immortalized cells (Soule et al., 1990). As shown in Figure 3.4C, cells grown without growth factors were significantly more resistant ($p<0.0001$) to NP-induced cytotoxicity at both 0.25 and 0.5 mM NP concentrations (56.3% and 19.4% viable, respectively) compared to cells grown in complete media (5.5% and 0.6%, respectively). Figure 3.4D verifies that MCF10 cell growth was significantly inhibited ($p<.0001$) by growth factor deprivation.

To further demonstrate the causal role of cell proliferation on the sensitivity to ZnO NP-induced cytotoxicity, experiments were performed using two different cell cycle inhibitors, Nocodazole and Colcemid. As shown in Figure 3.5A, rapidly growing T47D

cells were significantly more susceptible to NP toxicity than those treated with Nocodazole, an inhibitor that blocks cell cycle progression in the G_2 to M phase. For example, viability was 56% following 0.25 mM NP treatment in Nocodazole treated cells compared to 35% in rapidly dividing control cells (p=0.0047). A similar degree of protection from NP cytotoxicity was observed at higher 0.5 mM NP concentrations (22% vs. 7% viable, p=0.0367). PC3 cells treated with Nocodazole showed similar rescue at both NP concentrations, with viability at 52% vs. 69% (p<.0001) in untreated vs. treated (0.25 mM NP) cells, and 25% vs. 39% (p=.0405), respectively at 0.5 mM NP (Figure 3.5B).

Proliferation arrest in T47D breast epithelial cells using Colcemid also showed significant protection against NP-induced death. As shown in Figure 3.5C, cell viability in proliferating cells decreased twice as much in response to 0.25 mM NP treatment compared to non-dividing cells (25.4% vs. 50.2%, p= 0.0014). A similar protection against NP-induced cell death was observed using higher NP concentrations (0.5 mM), where 12.8% viability was observed in Colcemid treated cultures compared to 3.4% viability in control cultures. In Colcemid treated PC3 cells (Figure 3.5D), significant rescue was also seen at 0.25 mM NPs (~73% vs. ~92%, p=.022), with a similar trend occurring at 0.5 mM (~23% vs. 37%, p=.062). These data further support our hypothesis that susceptibility to NP-induced cytotoxicity is related to the proliferative capacity of the cell.

Our previous findings (Chapter 2) showed that neutralizing the ROS generated in response to NP exposure via chemical quenchers largely reversed the cytotoxicity in cells

of T lymphocyte lineage. Experiments shown in Figure 3.6 demonstrate that this same mode of rescue exists in other cell lineages (i.e., T47D breast and PC3 prostate epithelial cells). Breast cancer cells untreated with N-Acetyl Cysteine (NAC) were only ~56.4 and 34.1% viable at 0.3 and 0.5mM NP, respectively, while pretreatment with 5mM NAC rescued cells to ~100% and 91.3% viable (p= 0.0003 and 0.0026). Twice the concentration of NAC antioxidant resulted in 93.1 and 91.4% viability at the same NP concentrations (Figure 3.6A, p= .0018 and .0026). PC3 prostate cells also showed a dose-dependent pattern of rescue using NAC, with viability after NP treatment, increasing from 42.2% to 66.2% and 88.3% when treated with 2.5 or 5 mM NAC, respectively (Figure 3.6B, p= 0.0346 and 0.0002). Another antioxidant, glutathione (Glth), was tested at final concentrations of 1 and 2mM, and cells treated with 0.5 mM NP gained viability again from 42.2% to 56.9 and 87.4% for 1 and 2 mM Glth, respectively (Figure 3.6C). While a dose-dependent pattern of rescue was seen with Glth, only the highest concentration resulted in significant protection (p=0.0002). Collectively, these results suggest that ROS generation is a primary mechanism for NP toxicity for multiple cell types.

To assess whether ROS generation potentially contributes towards NP selectivity, experiments were performed using the Mitosox Red indicator dye to compare levels of NP-induced superoxide anion in primary versus cancerous T cells. Figure 3.7 shows significantly greater levels of NP-induced (0.3 mM) superoxide anion in cancerous cells compared to normal cells, which did not show significant ROS generation from untreated cells (p <.0001). In fact, 2.5 mM NP treatment, which could not be tested in the

cancerous cells due to complete toxicity, led to similar levels of ROS in normal T cells as observed at much lower NP concentrations (i.e., 0.3 mM) in cancerous T cells. These results suggest that cancer cells may be more susceptible to ZnO NP toxicity either because they generate more ROS in response to treatment, or they are less able to effectively neutralize ROS.

Recent studies have suggested that ZnO NP dissolve both extra- and intracellularly, and that zinc ions are responsible for mitochondrial disruption and subsequent ROS production (Xia et al., 2008). Another study showed that cell-NP contact was required for cytotoxicity, and that levels of $ZnCl_2$ comparable to NP treatments were not toxic to cells (Moos et al., 2010). In light of these differing opinions, the potential dissolution of our NP was evaluated by obtaining "NP supernatant" collected from the ZnO NP stock after 24h resuspension in media, followed by high speed centrifugation to remove NP aggregates. A zinc cation-specific indicator dye, Newport Green, was used to compare dissolution of ZnO NP to a standard curve generated using $ZnCl_2$, which is completely soluble at these experimental concentrations (Lide, 2009). A similar curve was observed using $ZnSO_4$ (data not shown). The levels of dissolved zinc cations derived from ZnO NP were significantly (20-25 fold, $p<.0001$) lower than those produced by $ZnCl_2$, with 10 mM ZnO NP showing equal fluorescence to the standard curve at ~0.45 mM $ZnCl_2$, and 1 mM ZnO NP showing approximately equal fluorescence to 0.045 mM $ZnCl_2$ (Figure 3.8A). Because 1 mM ZnO NP treatment results in complete Jurkat cell death (Figure 3.1A), which corresponds to ~.045 mM free zinc ions (Figure 3.8A), experiments were performed to determine it this level of free zinc ions contribute to the

NP toxicity. As shown in the inset to Figure 3.8A, no significant toxicity to Jurkat cells occurs at 0.05 mM $ZnCl_2$ (92.2% +/- 0.60% vs. 85.9% +/- 3.68%).

To directly assess the toxicity of NP-derived free zinc ions, Jurkat cells were treated with freshly prepared ZnO NP, or equivalent amounts of NP supernatant. As shown in Figure 3.8B, no significant loss in viability at any concentration of NP supernatant tested in contrast to the cytotoxicity of freshly prepared ZnO NP (58% viability at 0.25 mM, 14.3% viability at 0.5 mM). It is of interest to note that a modest hormetic effect of free zinc ions was observed in which an increase in viability was observed (88.7% vs. 101%), as described by others due to growth promoting effects of low concentrations of zinc ion (Calabrese and Baldwin, 2003). Nevertheless, these findings indicate that any ZnO NP dissolution that may occur prior to cell entry is insufficient to account for the NP-induced cytotoxicity observed in our experiments. Collectively, these results demonstrate that dissolution of our ZnO NP is minimal at physiological pH compared to readily dissolvable zinc salts.

To demonstrate that NP uptake is required for toxicity, Jurkat and T47D cells were treated with ZnO NP in the presence of a general endocytosis inhibitor, Cytochalasin D (Figure 3.9). Significantly greater viability was observed in inhibitor treated Jurkat cells unable to take up NP than cells capable of endocytosis (89.3 vs 68.9% at 0.25 mM NP, $p=.0160$) and (70.8 vs 29.0%, 0.5 mM NP, $p=.0002$), respectively. For T47D cells, significant protection was also observed at 0.5 mM NP treatment (66.3 vs. 41.4%, $p<0.0001$). It is important to note that the lower levels of NP-induced toxicity observed in these experiments relative to Figure 3.1 are likely due to the shortened

duration of NP treatment (12-16 h vs. 24 h) to preserve the effectiveness of Cytochalasin D. Filipin III, an inhibitor of lipid raft internalization, was also tested, and no rescue was seen suggesting that ZnO NP enter cells via a lipid raft-independent route (data not shown).

To investigate the role that surface charge has on NP toxicity in cancer cells, we used two sets of ZnO NP of the similar 4 nm size, but differing in electrostatic properties. One set (described as ZnO I) are positively charged, with a zeta potential of approximately +40 +/- 5 mV. The other (referred to as ZnO II) is closer to neutral in charge with a zeta potential of approximately +15 +/- 12 mV (Fig 3.10 B). Jurkat leukemia T cells were treated for 24 h with various concentrations of either ZnO I or ZnO II NP, and viability assessed via propidium iodide uptake. As expected, based on the typically high concentration of anionic phospholipids on the outer membrane and large membrane potentials of cancerous cells (Bockris and Habib, 1982; Papo et al., 2003; Abercrombie and Ambrose, 1962), positively charged ZnO I NP were significantly more toxic to Jurkat cells than neutral/negatively charged ZnO II NP (Figure 3.10A). At 0.3 mM concentrations, only 37.6% of the cells were viable compared to 69.1 % in ZnO II treated cultures ($p=.0025$). Similar trends were observed at higher 0.5 mM NP concentrations where 19.4% viability was observed with ZnO I compared to 62.4% with ZnO II NP ($p=.0002$).

Discussion

Results from this study demonstrate that several different types of cancerous cells have increased susceptibility to ZnO NP compared to normal cells of comparable lineage. The greatest differences in NP susceptibility were observed between hematopoietic cells, including B cells and T cells, where cancerous cells were killed at 22-40 fold lower NP concentrations compared to corresponding normal cells (Figure 2.1 and 3.1A). In addition, striking differences were observed between normal erythrocytes and their cancerous counterparts with erythroctyes remaining viable at concentrations 20 times the IC_{50} observed for erythroleukemic K562 cells (Figure 3.2). These results indicate that for nonadherent circulating cells of the blood system, cancerous cells display a much greater degree of susceptibility to ZnO NP-induced death than their normal counterpart cells.

However, when studies were extended to adherent cells of epithelial lineage, smaller differences in susceptibility between normal and cancerous cells were observed. The smaller therapeutic window for epithelial cells observed in our *in vitro* studies may be attributable to differences in experimental cell culture conditions between suspension and adherent cells. In adherent epithelial cells, a larger effective dose is likely experienced due to sedimentation of NP directly atop the monolayer, while freely suspended hematopoietic cell interactions are largely with unsettled suspended NP. In fact, sedimentation effects on ZnO NP cytotoxicity to monolayer cells have recently been reported in adherent fibroblasts (Heng et al., 2010). Additional factors may include the cell density as well the NP-to-cell ratio and NP-to-culture-surface-area ratio (Heng et al., 2010). Although factors of cell confluency and NP-to-culture-surface-area ratio were

controlled between the pairs of cancerous and normal cells in our study, we recognize that another potential confounding factor might include relative size differences between the cell types evaluated. For example, the relative lack of NP susceptibility between cancerous and primary prostate cells could be related to differences in their cell sizes affecting the relative NP dose per given cell given that PrEC primary cells were notably larger than PC3 cancer cells (data not shown). Although our results clearly demonstrate a high level of NP selectivity against cells of hematopoietic lineage, before a unified statement of selective toxicity against cancerous cells can be made, additional studies involving more cell types, 3D culture systems and carefully controlled cell densities, NP/culture surface area, and NP/cell surface area, as well as *in vivo* studies are needed. Nevertheless, at this stage of knowledge, experimental results suggest that ZnO NP may hold clinical promise for the treatment of hematological malignancies.

We hypothesized that susceptibility to NP toxicity is closely tied to the proliferative capacity of the cell. To test this hypothesis, experiments were performed to determine the extent to which the proliferation rates of cancerous and normal cells correlated with NP susceptibility. Notably, the highest degree of cancer cell selectivity was observed for cell lineages showing the greatest difference in proliferative potential. Quiescent primary T lymphocytes and erythrocytes showed at least ~27-35 fold greater resistance to ZnO NP than rapidly dividing T cell malignancies and erythroleukemic cells (Figure 3.1A and 3.2), and these cell types had that greatest differences in proliferative capacity (i.e., quiescent vs. ~ 23.6h for T leukemia and 23.3h for erythroleukemia). At the next level of the susceptibility spectrum, smaller differences

(1.88-fold) in IC_{50} between cancerous and normal breast epithelial cells were observed, which were paralleled by immortalized epithelial cells showing a corresponding faster, albeit slight, doubling time (~20%) relative to primary epithelial cells (Table 3.1). Although both cancerous and primary prostate epithelial cells showed nearly identical IC_{50} values, they also displayed nearly identical growth curves (Figure 3.3C). Thus, these results indicate that susceptibility to NP-induced toxicity parallels cellular proliferation rates, with the fastest growing cells typically displaying the greatest toxicity to ZnO NP. These findings also likely account for the greater disparity in IC_{50} seen in hematopoietic lineages than for epithelial cells.

Further experimental approaches designed to directly inhibit cell proliferation were used to show a causal role in protection against NP toxicity. MCF10A cells, which are a transformed yet non-cancerous epithelial cell line (Soule et al., 1990), can be stimulated to maximally proliferate by the addition of exogenous cholera toxin and epithelial growth factors. When this stimuli is removed and cell growth slowed, these cells became significantly more resistant to NP-mediated toxicity (Figure 3.4 C and D). A similar resistance to NP-induced toxicity was observed in slower growing serum-deprived Jurkat leukemia cells compared to rapidly growing Jurkat cells cultured in complete media (Figure 3.4 A and B). Similarly, breast and prostate cancerous epithelial cells were significantly more resistant to ZnO NP when proliferation was chemically halted using inhibitors that arrest cells in the mitotic phase of the cell cycle (Figure 3.5). These studies provide further evidence that increased susceptibility to ZnO NP-induced toxicity parallels the proliferative capacity of the cell. However, before ZnO NP can

potentially proceed toward future clinical chemotherapeutic applications, appropriate *in vivo* toxicity studies on rapidly dividing normal cells of the body, including bone marrow and gastric epithelial cells, are needed.

As generation of ROS is a well described general mechanism of NP toxicity in at least some cell types (Xia et al., 2006), experiments were performed to determine whether cancerous cells produce higher levels of NP-induced ROS compared to normal cells of corresponding lineage. We observed that cancerous T cells, when treated with NP, show significantly greater induction of ROS than primary T cells. An approximately eight times higher concentration of NP was required to induce comparable levels of ROS in primary T cells compared to leukemic cells (Figure 3.7). This may be due to greater NP uptake by cancer cells, greater mitochondrial disruption in cancer cells due to poor functioning, or less ability to metabolize ROS. Given the results of our proliferation studies, it is tempting to speculate that greater proliferation is tied to NP susceptibility through reactive oxygen species generation. Cells that are rapidly dividing have increased respiration and metabolism, and therefore higher levels of reactive oxygen species (Toyokuni et al., 1995; Szatrowski and Nathan, 1991). While cancer cells have intrinsically higher levels of ROS, they may not possess an equal ability as normal cells to handle further exogenous assaults from reactive oxygen species. This can translate into a greater susceptibility of cancer cells to drugs that induce ROS in cells (Trachootham et al., 2009). In fact, several anti-cancer drugs take advantage of this as a mechanism of action (Fang et al., 2007). Rescue via antioxidant pretreatment was also used to directly implicate ROS as the primary mechanism of NP toxicity in epithelial cancer cells (Figure

3.6) as a follow up on previous studies performed in leukemia cells (Hanley et al., 2008). Thus, NP-induced ROS appears to be a common consequence across cell lineages.

Recent studies have suggested that mitochondrial disruption by dissolved zinc cations contribute to intracellular ROS production and subsequent toxicity (Xia et al., 2008; George et al., 2010). Other research has shown that ZnO NP are capable of abiotic ROS production, which suggests that ROS are, at least in part, generated through a mechanism independent of dissolution (Song et al., 2010). Studies were performed to determine the extent to which our ZnO NP dissolve into free zinc cations and potentially contribute to the toxicity mechanism using the Newport Green DCF zinc indicator dye. We observed that NP prepared for use in cell culture experiments were at least 20-fold less soluble than $ZnCl_2$ salt, and that levels of dissolved zinc (from $ZnCl_2$) equivalent to that calculated for ZnO NP are not significantly toxic to cells. The effect of potential NP dissolution in the toxicity mechanism was further tested by preparing NP-free supernatant containing resulting dissolved free zinc cations. Studies demonstrated no significant toxicity from the NP supernatant in contrast to the expected cytotoxicity observed at corresponding concentrations of intact ZnO NP. Although these data collectively suggest that extracellular dissolution of ZnO NP is not the primary mode of toxicity, low levels of zinc ion release are likely. In addition, experiments indicated that active endocytic mechanisms are required for toxicity (Figure 3.9), suggesting that internalized NP would be subject to the acidic environment of the lysosome or endosome. In this intracellular location, appreciable dissolution of NP and release of free zinc ions may occur, resulting in mitochondrial disruption and subsequent ROS generation.

However, whether intra-organelle zinc ions play a major role in the ultimate toxicity mechanism will require future studies, and the outcome isn't a crucial determining factor for exploring the potential usefulness of NP in therapeutic applications. Nanoparticles benefit not only from the inherent selective toxicity toward hematopoietic malignancies, possibly through delivery of zinc cations to cells, but, unlike dissolved zinc, are also able to selectively target tumor sites via the enhanced permeation and retention (EPR) effect. Due to leaky vasculature and poor lymphatic drainage, NP tend to enter tumors easily from the bloodstream and become trapped, causing preferential accumulation at these sites (Cho et al., 2008). Further, NP can be modified to more effectively target cancerous cells, using antibodies for enhanced localization or through combination with existing therapeutics..

We further show that the charge on the surface of the nanoparticle is important for its toxicity to cancer cells. When NP are engineered to have reduced positive charge on the particle surface, the toxicity of NP appears to be reduced (Figure 3.10). This may be due to either reduced NP uptake by cells or decreased mitochondrial disruption by more neutral NP. In support of these possible modes of action, previous studies have shown that cancerous cells maintain more negative charges at the cell surface, which could facilitate greater uptake of positively charged NP by cancer cells (Abercrombie and Ambrose, 1962). It has also been shown that cancerous cells maintain a greater mitochondrial membrane potential, leading to targeting of this organelle by positively charged substances, leading to mitochondrial disruption and subsequent ROS generation (Trapp and Horobin, 2005). Regardless of the ultimate mechanism of action, these proof-

of-concepts experiments demonstrate that varying the electrostatic charge of NP can be one means to modify the cytotoxicity potential against target cells.

Conclusion

In this study, we demonstrate that ZnO NP show potential utility against hematopoietic malignancies, while additional studies are needed to more effectively compare NP toxicities for non-adherent vs. adherent cell types. The factors governing the toxicity of NP to certain cancer cells are assessed including proliferation potential, NP dissolution and surface charge, and ability to induce ROS differentially between cancerous and normal cells. Current work in our lab is focused upon further altering NP surface charge and doping NP in order to enhance their ability to produce reactive oxygen. With charge and targeting ligand modification, ZnO NP may display exciting potential as anticancer treatments.

References

Abercrombie, M. and Ambrose, E. J. (1962). The surface properties of cancer cells: a review. Cancer Res. 22, 525-548.

Al Nasiry, S., Geusens, N., Hanssens, M., Luyten, C., and Pijnenborg, R. (2007). The use of Alamar Blue assay for quantitative analysis of viability, migration and invasion of choriocarcinoma cells. Hum.Reprod. 22, 1304-1309.

Bockris, J.O.M. and Habib, M.A. (1982). Are there electrochemical aspects of cancer? J. Biol. Phys. 10, 227-237.

Bosanquet, A.G. and Bell, P.B. (2004). Ex vivo therapeutic index by drug sensitivity assay using fresh human normal and tumor cells. J. Exp. Ther. Oncol. 4, 145-154.

Calabrese, E.J. and Baldwin, L.A. (2003). Inorganics and hormesis. Crit. Rev. Toxicol. 33, 215-304.

Cho, K., Wang, X., Nie, S., Chen, Z.G., and Shin, D.M. (2008). Therapeutic nanoparticles for drug delivery in cancer. Clin. Cancer Res. 14, 1310-1316.

Coligan, J.E. (1995). Current Protocals in Immunology. (New York: Greene Publishing Associates and Wiley-Interscience).

Fang, J., Nakamura, H., and Iyer, A.D. (2007). Tumor-targeted induction of oxystress for cancer therapy. J. Drug Target. 15, 475-486.

Ferrari, M. (2005). Cancer nanotechnology: opportunities and challenges. Nat. Rev. Cancer. 5, 161-171.

George, S., Pohkrel, S., and Xia, T. (2010). Use of a rapid cytotoxicity screening approach to engineer a safer zinc oxide nanoparticle through iron doping. ACS Nano 4, 15-29.

Hanley, C., Layne, J., Punnoose, A., Reddy, K.M., Coombs, I., Coombs, A., Feris, K., and Wingett, D. (2008). Preferential killing of cancer cells and activated human T cells using ZnO nanoparticles. Nanotechnology 19, 295103.

Heng, B.C., Zhao, X., Xiong, S., Ng, K.W., Boey, F.Y., Loo, J.S. (2010). Cytotoxicity of zinc oxide (ZnO) nanoparticles is influenced by cell density and culture format.Arch. Toxicol. DOI:

Lanone, S. and Boczkowski, J. (2006). Biomedical applications and potential health risks of nanomaterials: molecular mechanisms. Curr. Mol. Med. 6, 651-663.

Lide, D.R. (2009-2010) CRC Handbook of Chemistry and Physics. (Boca Raton, FL: CRC Press).

McNeil, S.E. (2005) Nanotechnology for the biologist. J. Leukoc. Biol. 78, 585-594.

Moos, P.J., Chung, K., Woessner, D., Honeggar, M., Cutler, M.S., and Veranth, J.M. (2010). Zinc Oxide Particulate Matter Requires Cell Contact for Toxicity in human Colon Cancer Cells. Chem. Res. Toxicol. 23, 733-739.

Nel, A., Xia, T., Madler, L., and Li, N. (2006). Toxic potential of materials at the nanolevel. Science 311, 622-627.

Nie, S., Xing, Y., Kim, G.J., and Simons, J.W. (2007). Nanotechnology applications in cancer. Annu. Rev. Biomed. Eng. 9, 257-288.

Papo, N., Shahar, M., Eisenbach, L., and Shai, Y. (2003). A novel lytic peptide composed of DL-amino acids selectively kills cancer cells in culture and in mice. J. Biol. Chem. 278, 21018-21023.

Reddy, K.M., Feris, K., Bell, J., Wingett, D.G., Hanley, C., and Punnoose, A. (2007). Selective toxicity of zinc oxide nanoparticles to prokaryotic and eukaryotic systems. Applied Physics Letters. 90, 213902-213903.

Song, W., Zhang, J., Guo, J., Zhang, J., Ding, F., Li, L., and Sun, Z. (2010). Role of the dissolved zinc ion and reactive oxygen species in cytotoxicity of ZnO nanoparticles. Toxicol. Letters doi:10.1016/j.toxlet.2010.10.003.

Soule, H.D., Maloney, T.M., Wolman, S.R., Peterson, W.D., Brenz, R. Jr., McGrath, C.M., Russo, J., Pauley, R.J., Jones, R.F., and Brooks, S.C. (1990). Isolation and Characterization of a Spontaneously Immortalized Human Breast Epithelial Cell Line, MCF10. Cancer Res. 50, 6075-6086.

Stagsted, J. and Young, J.F. (2002). Large differences in erythrocyte stability between species reflect different antioxidative defense mechanisms. Free Radic. Res. 36, 779-789.

Szatrowski, T.P. and Nathan, C.F. (1991). Production of large amounts of hydrogen peroxide by human tumor cells. Cancer Res. 51, 794-798.

Toyokuni, S., Okamoto, K., Yodoi, J., and Kiai, H. (1995). Persistant oxidative stress in cancer. FEBS Lett. 358, 1-3.

Trachootham, D., Alexandre, J., and Huang, P. (2009). Targeting cancer cells by ROS-mediated mechanisms: a radical therapeutic approach? Nat. Rev. Drug Discov. 8, 579-591.

Trapp, S. and Horobin, R.W. (2005). A predictive model for the selective accumulation of chemicals in tumor cells. Eur. Biophys. J. 34, 959-966.

Xia, T., Kovochich, M., Brant, J., Hotze, M., Sempf, J., Oberley, T., Sioutas, C., Yeh, J.I., Wiesner, M.R., and Nel, A.E. (2006). Comparison of the abilities of ambient and manufactured nanoparticles to induce cellular toxicity according to an oxidative stress paradigm. Nano.Lett. 6, 1794-1807.

Xia, T., Kovovich, M., Liong, M., Madler, L., Gilbert, B., Shi, H., Yeh, J.I., Zink, J.I., and Nel, A.E. (2008). Comparison of the mechanism of toxicity of zinc oxide and cerium oxide nanoparticles based on dissolution and oxidative stress properties. ACS Nano 2, 2121-2134.

Zhi-Jun, Y., Sriranganathan, N., Vaught, T., Arastu, S.K., and Ahmed S.A. (1997). A dye-based lymphocyte proliferation assay that permits multiple immunological analyses: mRNA, cytogenetic, apoptosis, and immunophenotyping studies. J. Immunol. Methods. 210, 25-39.

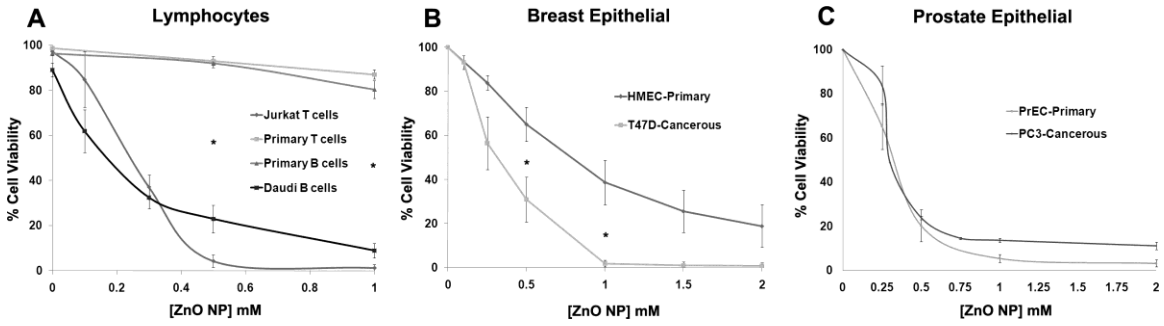

Figure 3.1. Differential cytotoxicity of ZnO NP. **A.** Immortalized Jurkat T cells and Daudi B cells, or normal primary T or B cells were treated with varying concentrations of ZnO NPs for 24 h and viability determined by PI uptake and flow cytometry. Data from three independent experiments is presented. **B.** Primary human mammary epithelial cells (HMEC; n=9) and T47D breast cancer cells (n=3) were plated in 24 well plates prior to NP treatment for 24 h, and cell viability assessed using the Alamar Blue assay. **C.** Primary Prostate Epithelial Cells (PrEC; n=4) and PC3 (n=3) cancerous prostate cells were plated and treated in the same manner described for the breast lines. For all figures, error bars depict standard error and asterisks indicate statistical significance as defined by $p<0.05$.. Data was analyzed using a repeated measures ANOVA and model based means post test.

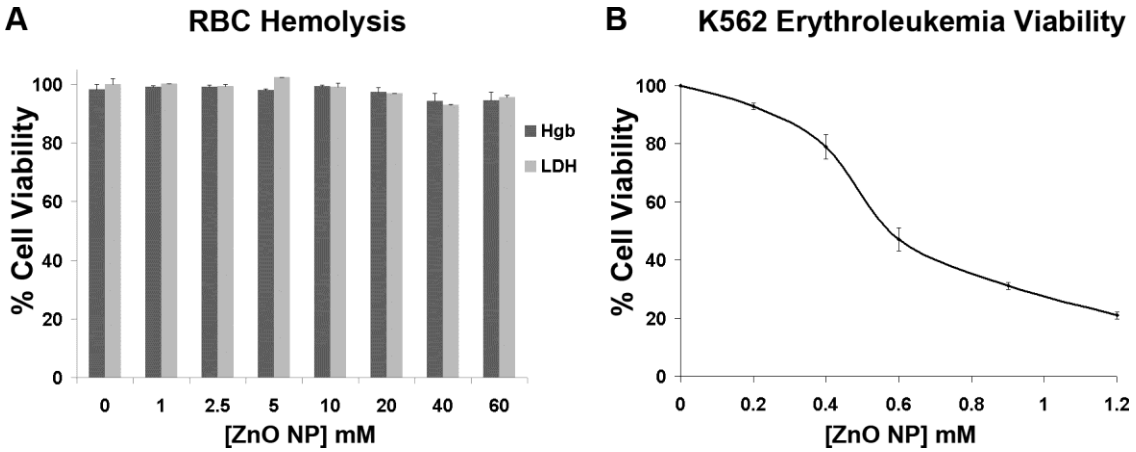

Figure 3.2. Erythrocyte susceptibility to ZnO NPs. **A)** Cells were incubated with 1-60 mM ZnO NP for 24 h and hemolysis determined based on the percentage of hemoglobin or LDH released relative to positive control cells completely lysed using 1% Triton-X. Data from three independent hemoglobin release experiments is depicted (dark colored bars). Data from a representative LDH assay performed in triplicate is presented with values normalized to % viability in control (NT) samples (light colored bars). **B)** Immortalized K562 erythroleukemia cells were plated at 1.2 x 10^5 cells/well and treated with NP for 24 h. Alamar Blue reduction was used to assess viability in four independent experiments. Error bars depict standard error.

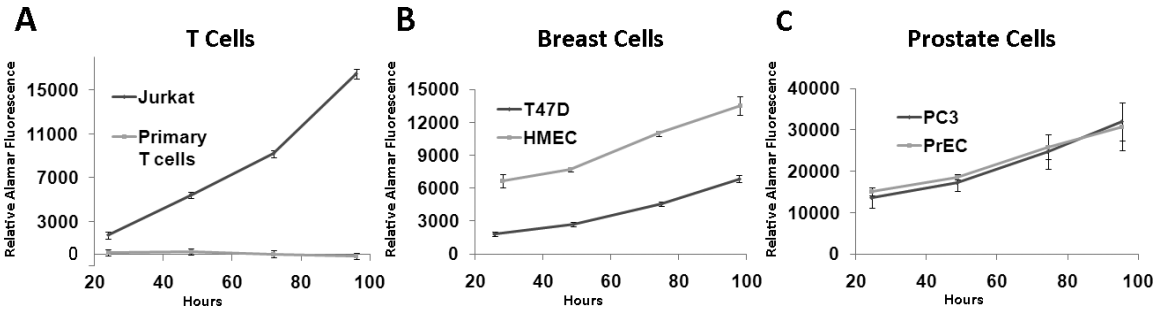

Figure 3.3. Proliferation rates of hematopoietic and epithelial cells. Cells were incubated for 4 hours with Alamar Blue each day (added at 10% total well volume each day) and fluorescence read using a spectrophotometer. A 4-day proliferation curve was generated for each cell type by plotting hours vs. fluorescence. **A** Cancerous and normal T cells were plated at 2 x 10^4 cells/well. **B.** Breast epithelial T47D cells were plated at 5 x 10^4 cells per well, while the larger HMEC were seeded at 1 x 10^4 per well to avoid confluence-induced growth inhibition. **C.** Prostate cells were plated identically to breast cells. For all panels, data from representative experiment performed in triplicate is shown. Cell doubling times were calculated as described in methods and shown in Table 1.

Table 3.1. Cell Proliferation Rate Compared with IC_{50} for ZnO Nanoparticles

Normal Cells			
Lineage		**Doubling Time (hrs)**	**IC_{50} (mM)**
Myeloid	Erythrocytes	quiescent	>10.0
Lymphoid	$CD4^+$ T cells	quiescent	>10.0
Epithelial	HMEC Breast	35.1 +/- 1.7	0.75
	PrEC Prostate	35.7 +/- 1.7	0.4
Cancerous Cells			
Lineage		**Doubling Time (hrs)**	**IC_{50} (mM)**
Myeloid	K562 Erythroleukemia	23.3 +/- 2.0	0.57
Lymphoid	Jurkat T	23.6 +/- 4.1	0.25
Epithelial	T47D Breast	29.3 +/- 1.1	0.3
	PC3 Prostate	35.3 +/- 1.3	0.4

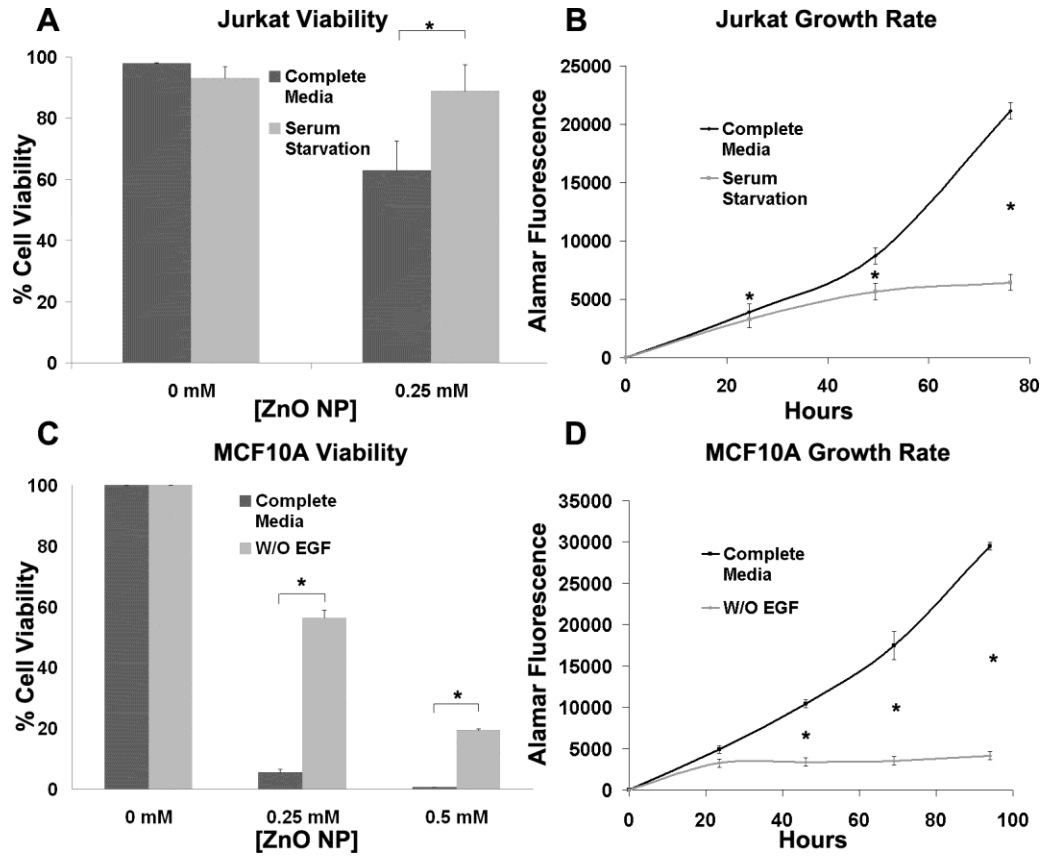

Figure 3.4. Effect of growth factor deprivation on susceptibility to ZnO NP toxicity. **A)** Jurkat cells (5 x 10^5 cells/mL) were incubated in standard media (10% FBS) or media containing only 2% FBS (serum deprivation) for 24 h, resuspended at 1 x 10^5 cells/well, and NP treated for 24 h. Viability was assessed by PI exclusion and flow cytometry. Data presented is from a representative experiment performed in triplicate. **B)** The inhibition of Jurkat T cell growth by serum starvation was verified by plating cells at 2 x 10^4 cells/well and Alamar Blue added each day at 10% well volume for 4 h. A curve of Alamar reduction fluorescence versus time was plotted from a representative experiment performed in triplicate. **C)** MCF10A cells were plated with or without epithelial growth factor (EGF) and cholera toxin, and effects of ZnO NPs (24 h) on cell viability determined using an Alamar Blue assay. Data from three independent experiments are presented. **D)** The inhibition of MCF10A cell growth was verified as described above (panel B) with data from a representative experiment performed in quadruplicate being presented. For all panels, error bars depict standard error and asterisks denote statistical significance ($p < 0.05$).

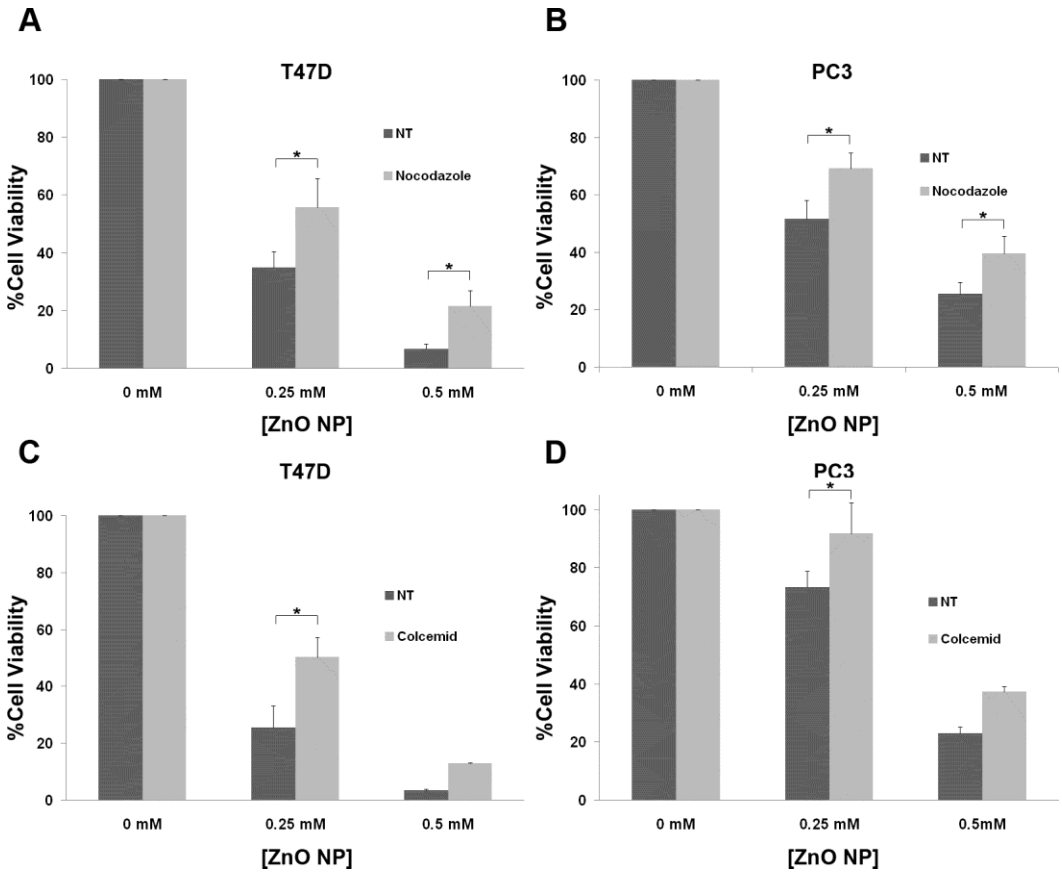

Figure 3.5. Effect of cell cycle inhibition on susceptibility to NP toxicity. **A,B** T47D cells were treated with 0.02μg/mL Nocodazole or 0.01 μg/mL Colcemid for 17 h. Cells were washed, cultured with fresh inhibitor-free media for 1-2 h, treated with NP for 24 h, and viability determined via Alamar Blue fluorescence. Data is presented from seven independent experiments (Nocodazole), or a representative experiment performed in triplicate (Colcemid). **C,D.** PC3 cells were treated with .02μg/mL Nocodazole or 0.008 μg/mL Colcemid, treated with NP for 24 h, and viability determined via an Alamar Blue assay. Five independent experiments are depicted for Nocodazole studies, and a representative experiment performed in triple is shown for Colcemid. For all panels, error bars depict standard error and asterisks denote statistical significance ($p<0.05$).

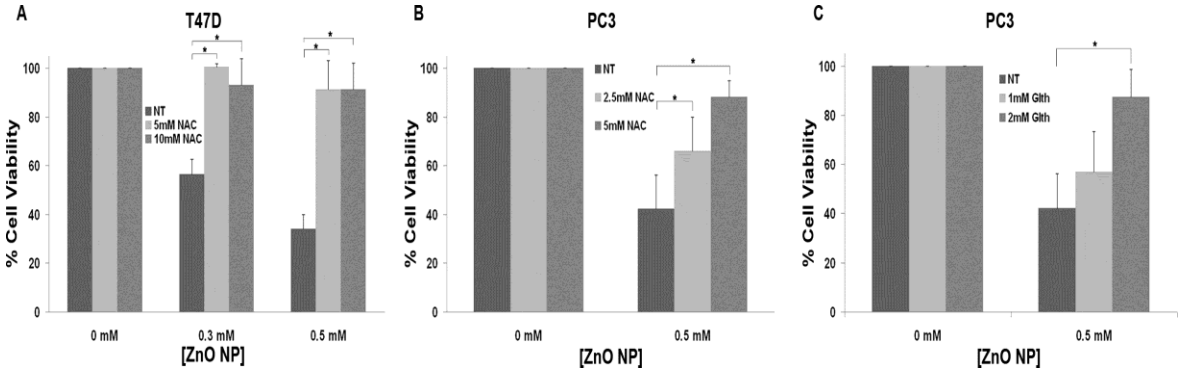

Figure 3.6. Effects of ROS on NP cytotoxicity. **A)** T47D cells were plated at 4 x 10^4 cells/well, allowed to adhere to well bottoms overnight, and then treated with 5 and 10 mM NAC for 1-2 h prior to treatment with NP for 24 h. Viability was determined as the percent reduction of Alamar Blue. Data presented is from three independent experiments with standard error and asterisks denoting significance. **B,C)** PC3 cells were plated in the same manner as T47D and pretreated with 2.5 or 5 mM NAC (B) or 1 or 2 mM Glth (C) before NP treatment and viability assessment as described above. Data from three independent experiments is depicted for both (B) and (C), and asterisks denote statistical significance.

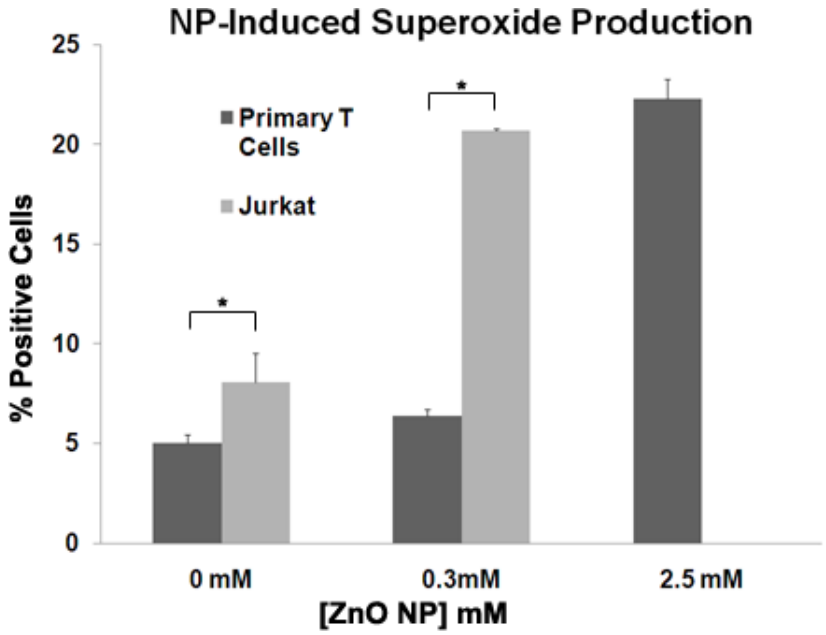

Figure 3.7. Superoxide induction by ZnO NP in primary vs. cancerous cells. Jurkat and primary T cells were plated at 1 x 10^5 cells/well and NP treated for 16-18 hrs. The fluorescence dye indicate Mitosox Red was added and flow cytometry used to assess superoxide anion production. A representative experiment performed in triplicate is presented with error bars depicting standard error and asterisks denoting statistical significance.

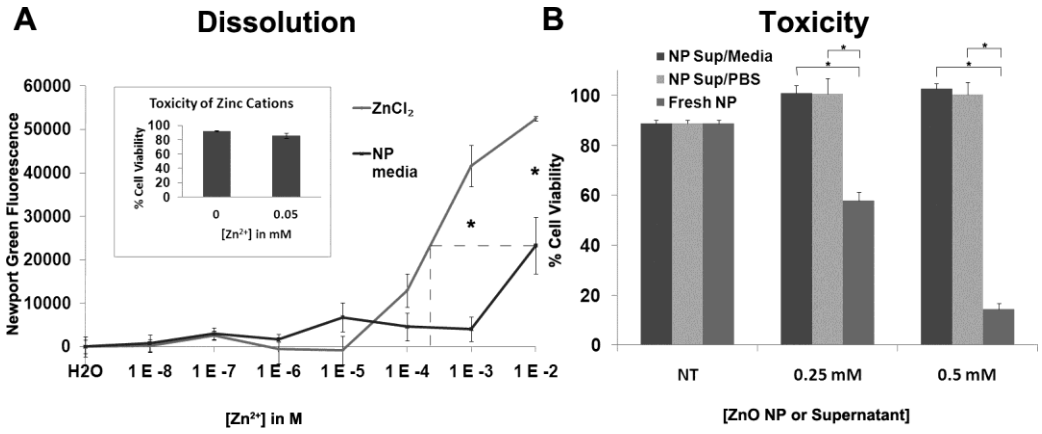

Figure 3.8. Dissolution potential of ZnO NP. **A)** To generate a standard curve for Zn^{2+} dissolution, $ZnCl_2$ was dissolved in deionized water at 10 mM and 0.2 mL serial 1:10 dilutions to 1 nM added to wells. ZnO NP were suspended at 10 mM in media and left to dissolve for 24 hrs. NP were subsequently centrifuged at 13,000 rpm for 20 min and serial 1:10 dilutions of supernatant (dissolved Zn^{2+}) made in the same range as the standard curve. Newport Green DCF (.1µM) was added to each well and fluorescence read on a spectrophotometer at 505/535 excitation/emission. Representative experiments performed in triplicate are depicted and asterisks denote statistical significance ($p<.05$). The dotted line indicates dissolution levels of 1 mM ZnO NP relative to the $ZnCl_2$ standard curve. Inset depicts toxicity of zinc cations from $ZnCl_2$ at concentrations equal to calculated dissolution levels for 1 mM ZnO NP. **B)** Effects of nanoparticle dissolution on toxicity. Nanoparticle stock solutions (50mM) were made in PBS or culture media, left 24 hours to dissolve, and centrifuged at 13,000 rpm for 20 min. NP supernatant or NP stock solutions were added to cells at equivalent concentrations, and PI uptake used to assess toxicity.

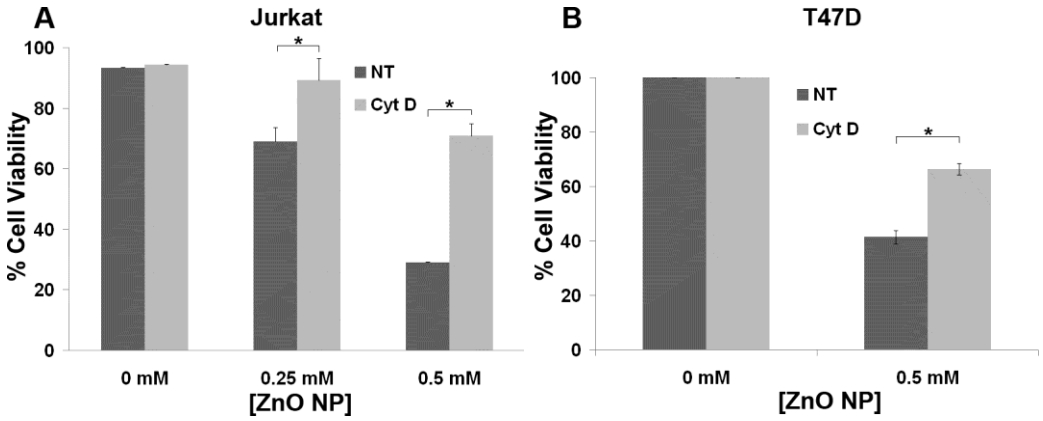

Figure 3.9. Effect of endocytosis inhibition on ZnO NP toxicity to two different cancerous cell types. **A**) Jurkat cells were pretreated with 1.5 µg/mL Cytochalasin D (Cyt D) for 2-3 h, plated at 1 E 5 cells/ well, and NP treated for ~16 h. Viability was assessed by PI staining and flow cytometry. Data presented is from a representative experiment performed in triplicate. **B**) T47D were plated at 2 E 4 cells/ well, allowed to adhere to bottom of wells, and pretreated with 1.5 µg/mL Cytochalasin D for 2-3 h. The inhibitor was removed, cells treated with NP for ~ 16 h and viability assessed using an Alamar Blue assay (n=5). Error bars depict standard error and asterisks denote statistical significance.

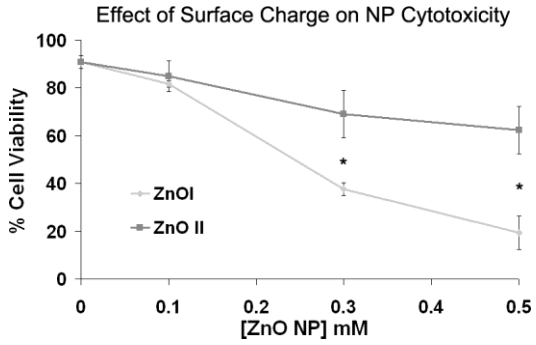

Figure 3.10. Effect of ZnO NP zeta potential on cytotoxicity. **A)** Jurkat cells were plated at 1 x 10^5 cells/well and treated with either 4 nm sized positively charged (ZnO I) or neutral (ZnO II) NPs for 24 h at 0.1, 0.3, and 0.5 mM. Viability was assessed using the PI exclusion assay and flow cytometry, n=3. Error bars depicted standard error and asterisks statistical significance as defined as $p<0.05$. Zeta potentials of 4 nm sized ZnO I and ZnO II NP were experimentally determined to be +40 +/- 5 mV and +15 +/- 12 mV, respectively (not shown).

CHAPTER 4: CONCLUSION

The study described herein was undertaken in two stages, and addressed as such in two separate chapters. This final chapter bridges the two studies and suggests future avenue of research.

Selective Toxicity

The second chapter explores the toxicity of ZnO NP to T cells of the human immune system, then further shows that the toxicity displays selectivity toward cancerous T cells relative to other hematopoietic cells evaluated. Importantly, the IC_{50} for ZnO NP is 28-35-fold lower in cancer cells than for normal T cells isolated from human blood. This selectivity was shown for both a T cell leukemia and lymphoma, Jurkat and Hut-78, respectively. Chapter 3 extends this work to cover another immune cell and its cancerous counterpart, primary B cells and Daudi B cell lymphoma. The third chapter also examines NP toxicity in cancerous and primary cells of epithelial origin from the prostate and the breast. Human mammary epithelial cells were compared with T47D breast carcinoma cells, and prostate epithelial cells were compared with the PC-3 prostate carcinoma line. It was found that cancerous B cells display similar susceptibility to NP cytotoxicity compared to normal B cells, much like the T cells previously examined. However, the differential toxicity seen between normal and cancerous cells of epithelial origin was much less striking. Breast cancer cells were significantly more susceptible

than were normal breast epithelial cells, but the difference between IC_{50} was around 2-3-fold. Cells of epithelial origin isolated from the prostate showed no significant resistance to NP cytotoxicity compared with prostate cancer cells. However, our research indicates that the relative lack of NP susceptibility between cancerous and primary prostate cells is related to their nearly identical growth curves in contrast to the markedly different growth rates observed between normal and cancerous hematopoietic cells, and the modest difference in proliferative potential between cancerous and normal mammary epithelial cells. The relative lack of difference in NP susceptibility observed in prostate cells could also be related to differences in cell size affecting the relative NP dose per given cell. Future experiments are planned to address this possibility as well as examining additional transformed and normal prostate cell isolates and additional cell lineages including lung cancers of both epithelial and fibroblast origin. In combination with alternate cell culture formats, including 3D cultures systems, these future studies will help determine if selective toxicity is dependent upon the cell lineage (hematopoietic, epithelial, or fibroblast) or reflect differences in NP exposure.

Cell Proliferation as a Mechanism for Selectivity

In light of the observed differential cytotoxicity of ZnO NP, experiments were performed in Chapter 3 to determine whether differences in cellular proliferation rates correlate with NP susceptibility. These experiments show that normal T cells have markedly slower growth rates than do cancerous T cells; in fact, no cell doublings occurred over three days, while leukemia cells doubled approximately every day. This is consistent with the known behavior of circulating immune cells in the literature, and is

expected to be true for B cells as well. Normal cells of epithelial origin, however, showed nearly similar proliferation rates as cancerous cells, with normal breast cells dividing slightly slower than cancerous, while no statistical difference was observed between growth rates of cancerous and normal prostate cells. This data correlates well with the difference, or lack thereof, in IC_{50} between cancerous and normal cells, suggesting proliferation as a mechanism for selective cytotoxicity.

To provide further evidence that rapid proliferation is among the causes of NP susceptibility, we directly inhibited the growth rate of cancerous cells of epithelial and hematopoietic lineage, both chemically and through serum deprivation. Leukemia cells became significantly more resistant to NP toxicity when proliferation was slowed through serum deprivation. A breast cell line, MCF10, which is immortalized but not cancerous, was cultured with and without Epithelial Growth Factor, and also displayed increased resistance when growth was slowed. Two chemical inhibitors that synchronize cells in mitosis were used in the breast and prostate cancer cells and both cell lines showed increased resistance using both inhibitors. Collectively, these data directly demonstrate that selective NP toxicity exists toward cells that divide rapidly, as cancer cells and some normal cells in the human body do. Thus, in vivo studies are needed to assess the overall toxicity profiles of ZnO NP to normal body cells and tissues.

Generation of Reactive Oxygen as a Mechanism for Toxicity and Selectivity

Chapter 2 of this work uses a general ROS indicator dye to show induction of reactive oxygen in cells upon NP treatment. Interestingly, lymphoma T cells showed greater increases of ROS production in response to NP exposure than that in normal T

cells. This is despite the much greater NP concentration used in primary T cells over lymphoma cells (5 mM vs. 0.5 mM). Chapter 3 uses primary T cells again, compared this time with leukemia cells, but employs a highly specific indicator dye, Mitosox Red, which detects only mitochondrial superoxide. Results were similar to those seen in Chapter 2, with eight times the concentration of NP treatment required to induce equal levels of superoxide in primary T cells as those seen in leukemia cells. This suggests that disruption of the mitochondrial membrane, and therefore electron transport, resulting in increased superoxide generation, is the ultimate toxic response of cells to ZnO NP. The higher levels of superoxide generated in cancer cells are likely due to an inability to neutralize excess reactive oxygen due to higher intrinsic oxidative stress inherent in cancer cells, resulting from increased proliferation/metabolism and greater mitochondrial instability. This was not shown experimentally here, but has been discussed extensively in existing literature.

Further experiments were performed to show that ROS generation is the ultimate toxic mechanism of NP in cancer cells. Pretreatment with the antioxidant N-Acetyl Cysteine showed dose-dependent and nearly complete rescue in leukemia cells (Chapter 2), as well as prostate and breast cancer (Chapter 3). A second antioxidant, Glutathione, was tested to confirm results, and showed similar rescue.

Nanoparticles as a potential clinical treatment benefit from their ability to be locally targeted to locations in the body where cancer cells densely populate; the generation of reactive oxygen may present the method through which NP can chemically target cancer cells.

Nanoparticle Dissolution

An important aspect to explore with respect to NP toxicity is their potential dissolution properties, both to estimate the tendency of these NP to accumulate in tissues and cells with repeated exposure, and to determine if toxicity occurs only upon dissolution. Experiments showed that after 24 hours, less than 10% of NP had dissolved to yield zinc cations relative to $ZnCl_2$ dissolution. In addition, levels of zinc ions calculated to result from NP dissolution at 1 mM were not toxic to cells, though this concentration of intact NP results in near complete cell death. Further experiments allowed NP to dissolve in suspension 24 hours, then centrifugation was used to pellet undissolved particles. Cells were treated with the supernatant from this suspension to determine if dissolved zinc cations directly from the NP were responsible for toxicity. Our studies collectively show that ZnO NP do not extensively dissolve acellularly, though it is possible that dissolution occurs after cell uptake. Other research, discussed in Chapter 3, suggests that zinc cations are the main culprit for toxicity; we speculate that while extracellular dissolution is not complete, low pH as is found in the lysosome may result in dissolution and release of free zinc, which then perturbs mitochondrial function, leading to generation of superoxide and subsequent cell death.

Cellular Uptake of Nanoparticles

Another important aspect of NP toxicity is assessment of cellular internalization. It is important to understand whether NP uptake is necessary for toxicity, and which routes are utilized by NP to enter the cell. We utilized one general inhibitor of endocytosis and a highly specific inhibitor of caveolae-mediated endocytosis to explore

possible routes of NP uptake. Cytochalasin D pretreatment, which depolymerizes actin, a molecule required for any cytoskeleton rearrangements needed to uptake molecules, resulted in significant rescue from NP toxicity in both leukemia and breast carcinoma cells. Both cell types were also pretreated with Filipin, which disrupts lipid raft dynamics and inhibits caveolin-dependent endocytosis, without significant effect on cytotoxicity (data not shown). This suggests an uptake method independent from caveolin. The data, while not pinpointing the exact mechanism for cellular uptake of NP, do demonstrate the necessity of NP uptake for cytotoxicity. This further supports the idea that dissolution, if any occurs, likely takes place in cellular compartments. Zinc cations, if released upon NP dissolution in media prior to uptake, would necessitate carrier proteins to our knowledge not inhibited by Cytochalasin D, to be distributed inside cells and cause mitochondrial superoxide production and resultant cell death. Nanoparticles may represent an exciting method for delivering zinc cations capable of inducing ROS production to cancer cells. Where zinc salts would dissolve in aqueous solutions and be cleared prematurely, NP appear to resist dissolution at least until cell entry and exposure to lower pH, liberating zinc cations to kill cells and being consumed in the process to avoid buildup.

Modification of Nanoparticles to Improve Selective Toxicity

We have shown that ZnO NP are more cytotoxic to cancer cells than to normal cells in several cell types; a logical next step is improvement of this selective toxicity toward cancer cells. We further show that increasing the positive charge on the NP surface increases cytotoxicity. Future modifications should include an addition of

targeting molecules, along with existing chemotherapeutic drugs to maximally enhance specificity and toxicity to cancer cells.

Conclusion

Collectively, this work has demonstrated the ability of zinc oxide NP to selectively kill certain types of cancer cells relative to their normal counterpart cells and explored characteristics of both NP and immortalized cells that contribute to the toxicity. In general, cancer cells appear to be more susceptible in a proliferation-dependent manner, and toxicity involves the generation of reactive oxygen species. This study describes the framework by which to explore the potential use of zinc oxide NP to treat hematological malignancies.